Termination of cell-type specification gene programs by miR-183 cluster determines the population sizes of low threshold mechanosensitive neurons

Changgeng Peng[1,§], Alessandro Furlan[2*], Ming-Dong Zhang[2*], Jie Su[2*], Moritz Lübke[2], Peter Lönnerberg[2], Hind Abdo[2], Jana Sontheimer[2]Erik Sundström[3], Patrik Ernfors[2,§]

[1] The First Rehabilitation Hospital of Shanghai, Tongji University School of Medicine, 200029 Shanghai, China.

[2] Department of Medical Biochemistry and Biophysics, Division of Molecular Neurobiology, Karolinska Institutet, 17177 Stockholm, Sweden.

[3] Department of Neurobiology, Care Sciences and Society. Karolinska Institutet, 171777 Stockholm, Sweden.

[§] *Corresponding Authors:* Changgeng Peng and *Patrik Ernfors*
E-mail: Changgeng.peng@tongji.edu.cn and *Patrik.Ernfors@ki.se*

*These authors contributed equally to this work.

Keywords: MiR-183-96-182, Shox2, dorsal root ganglia, sensory neuron, specification, fate switch

SUMMARY STATEMENT

In the Peng et al, a specific class of microRNAs is shown to determine the generation of two functionally different classes of touch sensitive primary sensory types by regulating timing of expression of a fate specifying transcription factor.

ABSTRACT

Touch and mechanical sensations require the development of several different kinds of sensory neurons dedicated to respond to certain types of mechanical stimuli. The transcription factor Shox2 (short stature homeobox 2) is involved in the generation of $TRKB^{+}$ low-threshold mechanoreceptors (LTMRs), but mechanisms terminating this program and allowing for alternative fates are unknown. Here, we show that the conditional loss of miR-183-96-182 cluster leads to a failure of extinction of Shox2 during development and an increase in the proportion of Aδ LTMRs ($TRKB^{+}$/$NECAB2^{+}$) neurons at the expense of Aβ slowly adapting (SA)-LTMRs ($TRKC^{+}$/$Runx3^{-}$) neurons. Conversely, overexpression of miR-183 cluster that represses Shox2 expression, or loss of Shox2, both increases the Aβ SA-LTMRs population at expense of Aδ LTMRs. Our results suggest that the miR-183 cluster determines the timing of Shox2 expression by direct targeting during development, and through this determines the population sizes of Aδ LTMRs and Aβ SA-LTMRs.

INTRODUCTION

Sensory neurons are heterogenous with some neuron types highly sensitive to stimuli and hence, display a low threshold to become activated. These register non-painful low threshold mechanical stimuli, and are therefore termed low-threshold

mechanosensitive neurons. Myelinated (A-fiber type) low threshold mechanoreceptors (LTMRs) terminate peripherally in the skin and participate in touch sensation. Interestingly, based on single-cell RNA sequencing, there are three types of myelinated LTMR: Aδ LTMRs, Aβ rapidly adapting (Aβ RA) LTMRs and Aβ slowly adapting (Aβ SA) LTMRs (referred to as NF1, NF2 and NF3 in (Usoskin et al., 2015)). Aδ LTMRs terminate as longitudinal lanceolate endings in hair follicles, and are involved in directional sensitivity and light touch. Aβ RA-LTMRs terminate as three morphologically distinct types of nerve-endings; in Meissner corpuscles in glabrous skin detecting movement across the skin, Pacinian corpuscles in glabrous skin tuned to high frequency vibration and lanceolate endings in hairy skin detecting movement and low-frequency vibration (Abraira and Ginty, 2013). Finally, Aβ SA-LTMRs terminate on Merkel cells in hairy and glabrous skin and are involved in sensitivity to skin indentation, and in addition - when terminating as longitudinal lanceolate endings in hair follicles - mediate hair deflection and touch sensation. These three types of can be defined by expression of NECAB2 and high levels of TrkB, (Aδ LTMRs), CALB1, RET and low levels of TrkB (Aβ RA-LTMRs) and finally, TrkC and RET (Aβ SA-LTMRs (Usoskin et al., 2015).

During development, touch sensitive neurons are specified from a common progenitor pool by a series of instructive signals and transcription factors (Lallemend and Ernfors, 2012; Liu and Ma, 2011). Early hybrid $TRKB^{+}$/$TRKC^{+}$ neurons diverge around E11-E12 in the mouse and eventually generates two mature *TrkB*$^{+}$ neuronal types, *TrkB*^{high} Aδ LTMRs and *TrkB*^{low} Aβ RA LTMRs both of which extinguish *TrkC* expression whereas those that maintain *TrkC* but extinguish *TrkB* expression become Aβ SA-LTMRs neurons (Bourane et al., 2009; Kramer et al., 2006; Lallemend and Ernfors, 2012). In contrast to the above touch sensitive neuron types, *TrkC*$^{+}$ proprioceptive mechanosensitive neurons express *Runx3*, which promotes the proprioceptive neuronal fate (Abdo et al., 2011; Kramer et al., 2006; Levanon et al., 2002; Scott et al., 2011).

MicroRNAs (miRNAs) can play a critical role during development. For example, one of the first miRNA identified, Lin-4, regulates developmental timing across different tissues in the nematode *C. elegans*, and loss of function mutations reiterate early developmental programs at inappropriate late larval stages (Chalfie et al., 1981; Lee et al., 1993; Wightman et al., 1993). For development of sensory systems, the MiR-183-96-182 (miR-183 cluster) is particularly interesting because it is expressed in many sensory organs such as retina, inner ear, dorsal root ganglion (DRG), olfactory epithelia and tongue epithelia in mouse (Bak et al., 2008; Lagos-Quintana et al., 2003; Lumayag et al., 2013; Sacheli et al., 2009). A high expression level of miR-183 cluster in retina is necessary for the development of its outer segments and functional maintenance in the adult (Busskamp et al., 2014a; Busskamp et al., 2014b; Lumayag et al., 2013; Zhu et al., 2011). MiR-183 cluster also regulates the development of sensory inner ear hair cells, and point mutations on *miR-96* affects hair cell function or hair cell development (causing progressive hearing loss in both mouse and human (Gu et al., 2013; Lewis et al., 2009; Mencia et al., 2009; Solda et al., 2012)). In this work, we conditionally delete miR-183 cluster in neural crest derivatives, including the DRG. We report that miR-183 cluster is expressed in DRG sensory neuron progenitors where it acts as a timer to extinguish *Shox2* through direct targeting its mRNA, and by this aborts the gene programs for Aδ NECAB2^{+}TRKB^{high} LTMR neurons and re-direct cell specification towards generation of Aβ TRKC^{+}RUNX3^{-} SA-LTMR neurons.

RESULTS

Loss of miR-183 cluster shifts the proportions of TRKB and TRKC neurons during embryonic development

All three miR-183 cluster members (*miR-183*, *miR-96* and *miR-182*) are specifically expressed in mouse DRG already at E10.5 and are continuously expressed through development into adulthood (Peng et al., 2017). To directly examine if miR-183

cluster plays a role in somatosensory neuron development, we crossed *Wnt1-Cre* mice (Danielian et al., 1998) with *miR-183-96-182*$^{flox/flox}$ mice (Peng et al., 2017) to generate *Wnt1-Cre; miR-183-96-182*$^{flox/flox}$ conditional knockout mice lacking miR-183 cluster in all DRG neurons (referred to as *miR*^{CKO} mice). *In situ* hybridization confirmed that expression of miR-183 cluster was depleted in DRG from E11.5 onwards in the *miR*^{CKO} mice (Fig. S1A). Immunohistochemical analysis of newly born (P0) mice revealed that the proportion of TRKB^{+} neurons was increased in the *miR*^{CKO} mice when compared to *Wnt1-Cre* mice (Fig. 1A-C). Importantly, the total number of neurons in L5 DRG was unchanged (Fig. 1D). In contrast, the percentage of TRKC^{+} neurons was decreased in the *miR*^{CKO} mice. This reduction was caused by a decrease in development of TRKC^{+}/RUNX3^{-} sensory neurons (Aβ SA-LTMRs) whereas TRKC^{+}/RUNX3^{+} proprioceptive neurons appear to be unchanged (Fig. 1E-G). Loss of miR-183 cluster had no effect at P0 on the proportions of TRKA (nociceptors), RET (some nociceptors and some LTMRs), neurofilament heavy polypeptide (NFH, all LTMRs), RET^{+}/NFH^{+} (RET^{+} LTMRs) and RET^{-}/NFH^{+} (all LTMRs except RET^{+}) in the *miR*^{CKO} mice when compared to *Wnt1*-Cre mice (Fig. S1B, C). These data suggest that loss of miR-183 cluster leads to fate-switch specifically of TRKC^{+} to TRKB^{+} neurons in the DRG without any changes in absolute numbers of LTMRs.

MiR-183 cluster controls the time window of Shox2 expression in DRG neurons

To identify the mechanism by which miR-183 cluster works to cause change of the fate of early DRG progenitor cells, we profiled RNA expression by RNA sequencing in three biological replicates of E12.5 lumbar DRG from the *miR*^{CKO} and control mice (Table S1^{Sheet1}). A total of 777 genes were significantly ($P<0.05$) up-regulated in the *miR*^{CKO} DRG when analysing the RNA sequencing data using Qlucore (Fig. 2A, Table S1^{Sheet2}). Among these, 101 genes were putative direct targets carrying binding site(s) for at least two members of miR-183 cluster predicted by TargetScan algorithm (http://www.targetscan.org, Table S1^{Sheet3}), and 38 out of the 101 genes were increased with more than 1.3 fold in the absence of miR-183 cluster (Fig. 2B, Table S1^{Sheet4}). Only two of these were transcription factors (Shox2 and Zbtb41), however,

Shox2 was among the top 10 highly expressed genes with more than 1.3 fold upregulation (Fig. 2C). This caught our attention, because Shox2 has been reported to be important for proper specification of TRKB$^+$ neurons in the developing DRG (Abdo et al., 2011; Scott et al., 2011). Furthermore, two highly conserved binding sites for *miR-183* and *miR-96* in the *Shox2* 3'UTR were predicted by TargetScan algorithm among many vertebrates (Fig. S2). Real time PCR independently confirmed that *Shox2* mRNA was increased 2.3-fold in the *miR^{CKO}* compared to control mice at E12.5 (Fig. 2D). SHOX2 protein was highly expressed in most DRG neurons at E10.5 and rapidly reduced at E11.5 and barely detected by E12.5 (Fig. 2E, F). TRKB$^+$ and TRKC$^+$ neurons segregate between E11.5 and E12.5 in the lumbar DRG (Kramer et al., 2006) and hence, SHOX2 repression precedes the diversification of these neurons types. SHOX2 extinction between E10.5 and E11.5 failed in *miR^{CKO}* mice, however, by E12.5 SHOX2 was downregulated similar to control mice (Fig. 2E, F). The finding that miR-182 was expressed in all DRG neurons throughout this developmental time window (Fig. 2G) indicates that this microRNA cluster works through determining the timing of extinction of SHOX2 rather than establishing selective expression in some but not other cells.

Extension of SHOX2 expression in TRKC$^+$ neurons in the *MiR^{CKO}* mice results in increased numbers of TRKB$^+$ neurons

Our results show that miR-183 cluster rapidly extinguishes SHOX2 expression at E11.5 in most neurons of the DRG. SHOX2 drives TRKB expression, and in the *Shox2* knockout mice there is a fate switch from TRKB$^+$ neurons to TRKC$^+$ LTMR neurons during this stage of development (Abdo et al., 2011; Scott et al., 2011). This opens for the possibility that miR-183 cluster could determine the proportion of TRKB and TRKC neurons generated during development by repression of *Shox2* expression. To obtain further insights into the development of LTMRs, we examined DRG at E10.5, prior to SHOX2 repression in most neurons. At this stage, TRKB and TRKC are largely co-expressed in DRG progenitors which a few days later diversify into TRKB$^+$ LTMRs and TRKC$^+$ neurons, as previously reported (Kramer et al.,

2006). Triple immunostaining for SHOX2, TRKC and TRKB showed that at E10.5, among TRKC$^+$ neurons virtually all also contains SHOX2 and among these, 24±3% also co-stain for TRKB. Furthermore, among TRKB$^+$ neurons, all were also TRKC$^+$ and SHOX2$^+$ (Fig. 3A). Thus, SHOX2 is expressed promiscuously both in all neurons expressing only TRKC as well as in all neurons expressing TRKB and these always co-express TRKC at E10.5 indicating that expression of TRKB is initiated in some of the TRKC$^+$/SHOX2$^+$ neurons. In the E11.5 wild-type mouse, TRKB and TRKC remained largely co-expressed although some neurons started to loose membrane presence of TKRC indicative of its downregulation, consistent with previous results (Kramer et al., 2006), and SHOX2 was expressed in the majority of the TRKB$^+$ neurons (Fig. 3B).

We next analysed control mice (*Wnt1-Cre*) and *miR*^{CKO} mice to determine how SHOX2 is expressed between E11.5 and E12.5 when TRKB$^+$/TRKC$^+$ neurons segregate into TRKB$^+$ and TRKC$^+$ neurons (Kramer et al., 2006), which defines the generation of different kinds of LTMRs (Abdo et al., 2011; Bourane et al., 2009; Scott et al., 2011). Immunohistochemical staining indicated the presence of more SHOX2$^+$ neurons and increased numbers of both TRKB$^+$/SHOX2$^+$ and TRKC$^+$/SHOX2$^+$ neurons at E11.5 (Fig. 3C). Quantification revealed in control (*Wnt1-Cre*) mice that SHOX2 expression among TRKB$^+$ neurons was reduced from 84±2% of all TRKB$^+$ neurons at E11.5 to 20±3% at E12.5. In contrast to maintained SHOX2 expression in some TRKB$^+$ neurons at E12.5, it was repressed in nearly all TRKC$^+$ neurons (Fig. 3D, F). Thus, SHOX2 segregates in TRKB but not TRKC expressing neurons. In *miR*^{CKO} mice, an increased percent of TRKB$^+$ neurons contained SHOX2 as compared to control mice at E11.5, but similar to control mice, only about a quarter of the TRKB$^+$ neurons contained SHOX2 at E12.5 (Fig. 3D). Because SHOX2 drives differentiation of the TRKB$^+$ LTMR fate, the shifted temporal repression of SHOX2 predict that the *miR*^{CKO} mice display an overall increased number of TRKB$^+$ neurons at E11.5. Quantification of the E11.5 DRG revealed that the *miR*^{CKO} mice had more TRKB$^+$/SHOX2$^+$ double positive neurons than control (*Wnt1-Cre*) mice whereas there was no change in the number of TRKB$^+$/SHOX2$^-$ neurons (Fig. 3E). This finding is in

line with that a failure of *Shox2* repression maintains TRKB expression in neurons that normally should have extinguished TRKB (e.g. $TRKC^+$ neurons). Consistently, the percent of $TRKC^+$ neurons containing $SHOX2^+$ was increased in the miR^{CKO} mice as compared to control *Wnt1-Cre* mice, with more than half of all $TRKC^+$ neurons expressing SHOX2 at E11.5 (Fig. 3F) while the total number of $TRKC^+$ neurons was unchanged (Fig. 3G), This shows that when miR-183 cluster is absent, SHOX2 is maintained in $TRKC^+$ neurons which normally should have lost SHOX2 by E11.5. We therefore conclude that that miR-183 cluster is critical for a timely extinction of SHOX2 expression at E11.5 when LTMR neurons diversify into distinct types.

Expression of miR-183 cluster and SHOX2 in the developing human DRG

Since the mature sequences of *miR-183, miR-96* and *miR-182* and their binding sites on *Shox2* 3'UTR are highly conserved among vertebrates, from lizard to human (Fig. S2 and data not shown), we next investigated if miR-183 cluster and TRKB, TRKC and SHOX2 are expressed in a similar way in the developing human as in rodents. Immunostaining on DRG sections from human embryos at post-conception time 6, 7, 8.5 and 11 weeks showed that TRKB, TRKC and SHOX2 are expressed in many neurons at 6 weeks with reduced number of neurons as development progresses (Fig. 4A-O). TRKB and TRKC sometimes were co-localized in 6 and 7 weeks old embryos (asterisk), while in 8.5 weeks-old embryos TRKB and TRKC neurons were largely segregated. This segregation was accompanied by a decline of SHOX2 in $TRKC^+$ neurons from 7 weeks to 8.5 weeks (Fig. 4F-O, arrows) and at 8.5 weeks, most of TRKC neurons had down-regulated SHOX2 (Fig. 4K-O). In contrast, TRKB was retained in $SHOX2^+$ neurons also at later embryonic stages (Fig. 4K-O arrow heads). In 11 weeks old embryos SHOX2 was exclusively expressed in $TRKB^+$ neurons (Fig. 4P), however, a few $TRKB^+$ cells were $SHOX2^-$ (inset in Fig. 4P). Expression of *Shox2* mRNA was also confirmed by reverse transcription PCR (RT-PCR) (Fig. 4Q). All together, these data show that expression of TRKB, TRKC and SHOX2 are similarly regulated in human and in mouse. *In situ* hybridization for miR-183 cluster suggested that all three miRNAs were expressed in DRG from 6 weeks to 8.5 weeks

human embryos (Fig. S3). Quantitative RT-PCR confirmed expression of miR-183 cluster, with *miR-182* expressed at the highest level (Fig. 4Q). *MiR-96*, which has a higher affinity for the human *Shox2* 3'UTR among the three miRNAs (see Fig. S2), showed the greatest regulation. *MiR-96* was first down-regulated to about 50% from week 5.5 to week 6, coinciding with elevated levels of *Shox2*. *MiR-96* was thereafter substantially increased at week 7, to levels slightly higher than at week 5.5 (Fig. 4Q). Our results evidence a similar development of TRKB and TRKC neurons and miR-183 cluster expression in the embryonic human as in mouse DRG.

MiR-183 cluster determines the adult proportion of Aδ LTMRs and Aβ SA-LTMRs

Our previous results show that miR-183 cluster participates in the diversification of $TRKC^+/RUNX3^-$ LTMR but not $TRKC^+/RUNX3^+$ proprioceptors (Fig. 1G). The only LTMRs expressing TRKC in the adult are Aβ SA-LTMRs (Usoskin et al., 2015). We therefore conclude that a miR-183 cluster dependent repression of TRKB participates in generating the $TRKC^+$ Aβ SA-LTMRs. However, it remained unclear if the increase of $TRKB^+$ neurons occurred in Aδ LTMRs and/or Aβ RA-LTMRs, because both types express TRKB (Usoskin et al., 2015). To examine if loss of miR-183 cluster results in persistent changes of the proportion of the different LTMRs and if so, which $TRKB^+$ LTMRs type(s) are involved, we collected and analyzed adult DRG from control (*Wnt1-Cre*) and the miR^{CKO} mice. Quantifying the total number of neurons revealed no differences between the genotypes (Fig. 5A) and consistent with analyses at P0, $TRKC^+$ neurons were reduced (Fig. 5B). Aβ RA-LTMRs and Aδ LTMRs are molecularly different and can be distinguished by expression of the calcium binding proteins CALB1 (Calbindin) in the former and NECAB2 in the latter. Quantification revealed no changes in the percent of all neurons expressing $TRKB^+/CALB1^+$ while $TRKB^+/NECAB2^+$ neurons were significantly increased (Fig. 5C-E). Thus, this suggests that miR-183 cluster is involved in diversification of a

TRKB^{+}/TRKC^{+} progenitor which segregates into the TrkB^{high}/NECAB2 Aδ LTMRs and TRKC^{+}/RUNX3^{-} Aβ SA-LTMRs.

MiR-183 cluster targets *Shox2* and efficiently extinguishes its expression in the DRG

To determine if *Shox2* is a direct target of miR-183 cluster, we cloned the mouse *Shox2 3*'untranslated region (UTR) which contains the two conserved binding sites for miR-183 cluster into a luciferase reporter vector (sensor) and co-transfected this vector together with an *miR-183-96* overexpression vector into HEK-293 cells (Fig. S4). Overexpression of *miR-183-96* repressed luciferase expression from the *Shox2 3'UTR* sensor vector by 58% and this repression was abolished when the conserved seed sequences of *miR-183-96* binding sites in the sensor vectors were mutated (Fig. 6A, B). Since there is only one nucleotide difference between the seed sequence of miR-182 and that of miR-96, we examined if also miR-182 can target *Shox2* 3'UTR. Co-transfection of a miR-182 overexpression vector repressed the luciferase expression from the *Shox2 3'UTR* sensor vector by 43%, and this repression could be fully rescued by mutating the miR-96 binding site on the sensor vectors (Fig. 6A, B). These results show that miR-183 cluster regulates the expression levels of *Shox2* by directly binding to the conserved binding sites located within the 3'UTR. To confirm that miR-183 cluster can represses *Shox2* expression *in vivo*, we forced expression of *miR-183-96* in chicken DRG by electroporating a *pCAG-miR-183-96-IRES-GFP* vector into the neural tube at the HH13 stage. Embryos were allowed to continue to develop and were analyzed at E7.5, when the neural crest cells have migrated, undergone neurogenesis and coalesced to form the DRG. Quantification showed that the percentage of GFP^{+}/SHOX2^{+} cells over total GFP cells was dramatically reduced in the *miR-183-96* overexpressing group as compared to the control *pCAG-IRES-GFP*-electroporated group (Fig. 6C). These results suggest that the miR-183 cluster can target the Shox2 mRNA.

MiR-183 cluster diversify TRKB$^+$ and TRKC$^+$ mechanosensory neurons through regulation of *Shox2*

Based on the strong correlation between upregulation of SHOX2 and changed proportions of subgroups of DRG neurons in the *miR^{CKO}* mice, we next investigated whether SHOX2 represents the key target of miR-183 cluster responsible for the phenotype in the *miR^{CKO}* mice by using gain-of-function and loss-of-function strategies. Thus, if miR-183 cluster works through repression of *Shox2*, overexpression of SHOX2 is expected to phenocopy the *miR-183^{CKO}* mice and genetic ablation of Shox2 is expected to lead to the reverse phenotype. Overexpression of Shox2 resulted in more than a 2-fold increase of TRKB$^+$ DRG neurons in chicken embryos (Fig. 6D, E). Crossing *Wnt1-Cre to Shox2$^{flox/flox}$* mice (Abdo et al., 2011) to generate *Wnt1-Cre;Shox2$^{flox/flox}$* mice that have a loss-of-function of *Shox2* in the DRG revealed a marked reduction of TRKB$^+$ DRG neurons and increased number of TRKC$^+$ DRG neurons at P0, as previously reported (Abdo et al., 2011; Scott et al., 2011) (Fig. 6F-H). Moreover, we found that the TRKC$^+$/RUNX3$^-$ but not TRKC$^+$/RUNX3$^+$ neuron types were increased in the *Wnt1-Cre;Shox2$^{flox/flox}$* mice as compared to the *Shox2$^{flox/flox}$* control mice (Fig. 6G, H). Altogether (see Fig. 6I), our results suggest that miR-183 cluster works through regulation of *Shox2* in a gene-regulatory network (Fig. 6J) determining the population sizes of Aδ LTMRs and Aβ SA-LTMRs generated during development.

DISCUSSION

This study represents to our knowledge the first molecular identification and characterization of a miRNA that determines the timing of expression of fate-inducing transcription factors in primary sensory neurons. We show that the miR-183 cluster

terminates genesis of Aδ LTMRs neurons in favour of Aβ SA-LTMR neurons during development through extinction of *Shox2* expression.

Expression of neurotrophic factor receptors confers ligand sensitivity. Neurotrophic factor signaling plays critical roles during development for neuron survival, axon growth, peripheral target innervation, patterns of terminations in the spinal cord as well as differentiation into specialized and modality-specific sensors (Lallemend and Ernfors, 2012; Marmigere and Ernfors, 2007). Consequently, expression of growth factor receptors is one of the first distinguished features during cell type diversification in the DRG. However, distinct transcription factor programs are involved in this process, and often interact with growth factor receptor signaling. RUNX3 is critical for the specification of TRKC expressing proprioceptive sensory neurons (Levanon et al., 2002) where both BRN3A and RUNX3 are important for repression of TRKB to generate RUNX3^{+}/TRKC^{+} proprioceptive neurons (Dykes et al., 2010; Kramer et al., 2006). While RUNX3 suppresses *Shox2* expression, *Shox2* is unable to suppress *Runx3* (Abdo et al., 2011). Therefore, initiation of *Runx3* seems to be contributing both by the suppression of alternative fates as well as for the initiation of the proprioceptive neuron fate. Because of this, neither *Shox2* nor miR-183 cluster are expected to affect proprioceptive neuron development. This agrees with our results, revealing no effect on TRKC^{+}/RUNX3^{+} neurons in both the *miR^{CKO}* mice and the *Shox2* CKO mice at P0. Consequently, these findings predict miR-183 specifically to affect LTMR neuron development involved in touch.

Some neurons acquire RET expression already at E10.5 in the mouse (Molliver et al., 1997), thus coinciding with segregation of other types of LTMRs (eg. TRKB^{+} and TRKC^{+}/RUNX3^{-} neurons). These neurons depend on RET signaling for the specification of RA-LTMRs (Bourane et al., 2009; Honma et al., 2010; Lecoin et al., 2010; Luo et al., 2009). We found no change in total RET^{+} neurons, nor in myelinated NFH^{+}/RET^{+} neurons at P0. Therefore, our findings predict that miR-183 primarily affects LTMRs other than early RET^{+} neurons which differentiate into Aβ RA-

LTMRs. Thus, it seems that RET$^+$ RA-LTMRs as well as TRKC$^+$/RUNX3$^+$ proprioceptors rely on mechanisms independent of miR-183 cluster.

Consistent with distinct paths for diversification, TRKB$^+$ Aδ LTMRs and TRKC$^+$ Aβ SA-LTMRs seem to emerge from hybrid TRKB$^+$/TRKC$^+$ neurons through extinction of TRKB (Kramer et al., 2006). SHOX2 has been shown to be necessary for proper diversification of TRKB$^+$ neurons, and in its absence, up to 60% of TRKB$^+$ neurons lost its expression, while TRKC$^+$ neurons increase (Abdo et al., 2011; Scott et al., 2011). In this study, we find that this increase of TRKC$^+$ neurons occurs among TRKC$^+$/RUNX3$^-$ neurons differentiating into LTMRs. SHOX2 therefore participates specifically in the split between neurons that differentiate into Aδ LTMRs and Aβ SA-LTMRs. In this process, the timing of SHOX2 extinction rather than the selective expression in particular cells between E10.5 and E11.5 through miR-183 cluster repression of *Shox2* opens for the emergence of more TRKC$^+$ LTMR neurons which eventually become Aβ SA-LTMRs.

Given the fact that all subtypes of sensory neurons in DRG come from the same progenitor pool derived from trunk neural crest cells, the inversely proportional changes between two related neuron types indicate a shared genetic pathway fating one type and repressing the other. This conclusion is generalized, as numbers do not always add up perfectly. For example, at P0, the percentage increase of TRKB$^+$ neurons is less than the increase of TRKC$^+$ neurons. Thus, this opens for cell fate changes or loss of cells not recorded in this study. Nevertheless, *Shox2* is a direct target for miR-183 cluster, and the de-repression of *Shox2* in the *miR-183^{CKO}* mice appears to be the main mechanism causing the phenotype. Consistent with this, in the *Shox2* CKO mice TRKB$^+$ neurons decrease and TRKC$^+$ neurons increase while in the *miR-183^{CKO}* mice TRKB$^+$ neurons increase similar to *Shox2* overexpression, and TRKC$^+$ neurons decrease. Furthermore, the major phenotype of the *miR-183^{CKO}* mice and *Shox2* CKO mice encompasses these neuron types, which differentiates into Aδ LTMRs and Aβ LTMRs.

Pre-mi-RNAs are processed to become mature miRNAs by the ribonuclease Dicer (Bernstein et al., 2001; Zhang et al., 2004). While, system-wide deletion of *Dicer* leads to early embryonic lethality (Bernstein et al., 2003), conditional deletion restricted to the peripheral nervous system reveals its indispensable role for cell survival, development and plasticity in the nervous system (Fiorenza and Barco, 2016). In the DRG, loss of *Dicer* results in abnormal development with marked loss of sensory neurons and a failure to produce axonal projections (Zehir et al., 2010). The miR-183 cluster is contained within an -4kb genomic sequence, and produced as a polycistronic pri-miR transcript (Dambal et al., 2015) and have related seed sequences (Karali et al., 2007; Ryan et al., 2006; Xu et al., 2007). *MiR-183* is down-regulated in animal models for neuropathic pain and knee joint osteoarthritis (Li et al., 2013; Lin et al., 2014) and consistently, forced *miR-183* expression by intrathecal injections of lentivirions attenuate spinal nerve ligation-induced mechanical allodynia (Lin et al., 2014). Furthermore, loss of miR-183 cluster function in the adult results in increased basal mechanical sensitivity and mechanical allodynia (Peng et al., 2017). Interestingly, the increased allodynia during nerve damage involves $TRKB^{+}$ Aδ LTMRs (Peng et al., 2017). However, this effect of miR-183 cluster-deficiency is caused by increased sensitization/excitability due the loss of a continuous suppression of auxiliary voltage-gated calcium channels subunits (*Cacna2d1 and Cacna2d2*) in adult mice. Thus, while miR-183 cluster targets *Shox2* during development affecting cell-type specification, *Cacna2d1* and *Cacna2d2* are targeted in adult affecting mechanical sensitivity. This miRNA cluster therefore serves different functions in sensory neurons during development, as compared to adult.

Given that miR-183 cluster and many of its target genes are highly conserved in mammalians it is believed that miR-183 cluster could play similar roles in human as in mouse. This prediction is enforced by the discovery that a point mutation in miR-96 causes progressive hearing loss in both mouse and human (Lewis et al., 2009;

Mencia et al., 2009; Solda et al., 2012). Our data show that miR-183 cluster is also highly expressed in the developing DRG of humans along with the direct target gene *Shox2*. These data indicate that miR-183 cluster play similar roles in the developing human DRG as it does in the mouse.

MATERIALS AND METHODS

Mutant mice

MiR-183-96-182$^{flox/+}$ mice (Peng et al., 2017) were crossed with *Wnt1-Cre* 129/SvEv mice (Danielian et al., 1998) to obtain *Wnt1-Cre; Mir-183-96-182*$^{flox/+}$ mice. *Wnt1-Cre; Mir-183-96-182*$^{flox/+}$ mice were mated to *Mir-183-96-182*$^{flox/+}$ mice to obtain *Wnt1-Cre; Mir-183-96-182*$^{flox/flox}$ mice and *Wnt1-Cre* control mice. *Wnt1-Cre; Shox2*$^{flox\,/\,flox}$ mice were obtained by crossing *Shox2*$^{flox\,/\,flox}$ mice (Cobb et al., 2006) with *Wnt1-Cre* mice (Danielian et al., 1998), and the Genotyping of the *Shox2* floxed allele and *Wnt1-Cre* was performed as previously described (Abdo et al., 2011). Timed pregnant females were used for collection of embryonic stages; noon of the day of vaginal plug detection was designated as E0.5. All animal work was conducted under ethical permission from the Swedish ethical review panel, norra djurförsöksetiska nämnden.

Human tissue

Human embryonic and fetal tissue was retrieved from elective routine abortions at the Karolinska University Hospital with written consent from the pregnant women， and DRGs were dissected and immersed in 4% PFA for 6 hours, further immersed in 20% Sucrose over night after wash in PBS for 5 minutes, finally embedded in OCT and sectioned in thickness of 14μm. Age (weeks after conception) of the aborted tissue was determined using anatomical landmarks (England, 1990; Yamada and Takakuwa, 2012). Use of human fetal tissue was approved by the Stockholm vetting board on ethics in human research (2007/1477-31, 2011/1101-32, 2013/564-32).

In situ hybridization and histology

Paraffin sections (8 μm) and cryosections (14 μm) from lumbar mouse and human DRG were processed and hybridizations were performed as described in (Peng et al., 2012). Digoxigenin (DIG)-labelled LNA probes for *miR-183* (Exiqon, Denmark) and *miR-182* (Exiqon, Denmark), and DIG-labelled RNA probe (Pengekiphen, Suzhou,

China) for *miR-96* were used. Alkalin-phosphatase-conjugated anti-digoxigenin antibody (Roche, 1: 2000) was used and Alkaline phosphatase staining was developed with Fast Red (Roche) and then followed by counterstaining with DAPI or immunostaining for ISL1 (clone 39.4D5; Developmental Studies Hybridoma Bank (DSHB), The University of Iowa, Iowa City, USA, 1:100). Images were taken using an Olympus FV1000 confocal microscope.

Immunostainings

Immunostainings on 14 µm cryosections from mouse and human lumbar DRG was performed as previously described (Abdo et al., 2011). The following primary antibodies were used: mouse antibodies against ISL1 (DSHB, USA, 1:100), SHOX2 (Santa Cruz, USA, 1:400), NFH (neurofilament, heavy polypeptide) (CloneN52; Sigma-aldrich, St. Louis, MO, USA, 1:500); rabbit antibodies against RUNX3 (gifts from Thomas Jessell, Columbia University Medical Center, 1:300), ISL1 (gifts from Thomas Jessell, Columbia University Medical Center, 1:250), NFH (Millipore, USA, 1:200), TRKA (Millipore, USA, 1:500), TRKC (Cell signaling, USA, 1:500), NECAB2 (Proteintech Europe, 1:1000), CALB1 (Millipore, USA, 1:500) and chicken-TRKB (kind gift from Louis F. Reichardt, 1:2000); goat antibodies against TRKA (R&D systems, Minneapolis, MN, USA, 1:500), TRKB (R&D systems, Minneapolis, MN, USA, 1:500), TRKC (R&D, 1:500), Ret (R&D, 1:100) and GFP (Abcam, USA, 1:500); Guinea pig antibodies against TLX3 (kind gift from Carmen Birchmeier). Secondary antibodies were fluorescently labeled (AlexaFluor 405/488/594/647; Molecular Probes, Invitrogen, USA). Fluorescent images were taken with a confocal laser scanning microscope (Olympus FV1000 confocal microscope or Zeiss LSM700), and processed with Adobe Photoshop CS software.

Quantification methods

All markers were counted on DRG sections at either lumber level 4-6 (*Wnt1-Cre* control and miR^{CKO} mice) or brachial level (*Wnt1-Cre;* $Shox2^{flox/flox}$ and $Shox2^{flox/flox}$ mice). $TRKA^+$, $TRKB^+$, $TRKC^+$ and $SHOX2^+$ cells were counted on 8 position-

matched sections from each *Wnt1-Cre* control and *miR*^{CKO} embryo at E11.5 stage. To analyze the proportion of each marker at P0 stage, the numbers of TRKA^{+}, TRKB^{+}, TRKC^{+}, RUNX3^{+}, RET^{+} and NFH^{+} cells were counted on at least the three biggest sections from three DRG per each *Wnt1-Cre* control, *miR*^{CKO}, *Wnt1-Cre; Shox2*$^{flox/flox}$ and *Shox2*$^{flox/flox}$ mouse, then normalized to the number of total neurons (ISL1^{+} or TLX3^{+}) on the same sections. To get the numbers of total neurons in L5 DRG at P0 (ISL1^{+}) and adult (TLX3^{+}), every ninth serial section through L5 ganglion was counted, then multiplied by 8 to get the number of total neurons in L5 DRG. TRKB^{+}, CALB1^{+}, NECAB2^{+}, TRKC^{+}, TRKA^{+} and NFH^{+} cells were counted on every ninth serial section through L5 ganglion of *Wnt1-Cre* control and the *miR*^{CKO} adult mice (5-6 months), and the number of each marker was then normalized to the number of TLX3+ neurons to get its proportion. All values shown are mean ± SEM. Statistical significance between groups was assessed by *t*-tests using GraphPad Prism 5. A value of $P < 0.05$ was considered significant.

Expression profiling of DRG

Mouse lumbar DRG tissue was dissected from E12.5 three controls (two *Wnt1-Cre* and one *WT*) and three *miR*^{CKO} embryos. Total RNA was isolated using Trizol Reagent (Invitrogen) and processed with TruSeq Stranded mRNA Sample Prep Kit (Illumina/USA) to get the cDNA library according to the manual. The adapter-ligated libraries were sequenced on the Illumina sequencer according to the manufacturer's instructions. Read processing was performed as described (Islam et al., 2014), except that the molecule counting by unique molecule identifiers was omitted. Alignments against UCSC mm10 genome were made with bowtie1 version 0.12.9 (Langmead et al., 2009) allowing for up to 3 mismatches. RPKM values were obtained by dividing each read count by the transcript length in kilobases and normalizing to a total of 1 million in each sample. Profiling data from mouse DRG (Table S1^{sheet1}) were then analysed using Qlucore Omics Explore, and significantly (P<0.05) upregulated genes (Table S1^{sheet2}) in the *miR*^{CKO} DRG were matched to the targets (Table S1^{sheet3})

predicted by TargetScan algorithm. The 38 overlapped genes with upregulation more than 1.3 fold were listed in Table S1[Sheet4].

Vector constructs

The genomic sequences (shown in Table S1[Sheet5]) for *miR-183-96* and *miR-182* were synthesized and cloned into *pCAGIG* vector (Addgene/USA, #11159). Levels of *miR-183, miR-96* and *miR-182* expression from the OE vectors *pCAG-miR-183-96-IRES-GFP* and *pCAG-miR-182-IRES-GFP* were quantified by real time RT-PCR after transfection into HEK-293 cells (Fig. S4). The mouse *Shox2* 3'UTR (Entrez Gene Acc. No. NM_001302357.1) was amplified from cDNA of E12.5 DRG with the primers indicated in Table S1[Sheet6], and cloned into the *Xba*I site downstream of the Luciferase CDS in the *pGL3 promoter* vector (Promega, USA) to obtain *pGL3-Shox2-3'UTR* vector. Binding site-mutated *Shox2* 3'UTR sequences were directly synthesized and cloned into *pGL3 promoter* vectors. Truncated mouse *Shox2* CDS (position 210-1350, without binding sites for miR-183 cluster, Entrez Gene Acc. No. NM_013665.1) was subcloned from pGEMT-Shox2 cDNA plasmid (gift from J. Cobb, University of Calgary) into *pCAGIG* vector to obtain *pCAG-Shox2-IRES-GFP* OE vector.

Luciferase reporter assays

The miRNA sensor assays were conducted in HEK293 cells co-transfected with 500 ng/well *pGL3-Shox2-3'UTR* sensor vector and 10 ng/well *pRL-SV40* (internal transfection control) along with 1 µg/well *pCAG-miR-183-96-IRES-GFP* vector or 1 µg/well *pCAG-miR-182-IRES-GFP* vector using Lipofectamine 2000 (Invitrogen). The corresponding rescue assays were done in HEK293 cells co-transfected with 500 ng/well *pGL3-mut-Shox2-3'UTR* sensor vector with 1 µg/well *pCAG-miR-183-96-IRES-GFP* vector or 1 µg/well *pCAG-miR-182-IRES-GFP,* and 10 ng/well *pRL-SV40* vector. Cells were lysed in Passive Lysis Buffer 40 hrs post-transfection, and Firefly and Renilla Luciferase luminescence was measured in a Victor™ luminometer (Wallac Sverige/Sweden) using the Dual-Luciferase® Reporter Assay system

(Promega) according to the manufacturers' instructions. Firefly luminescence was normalized against Renilla luminescence for each well. Assays were performed in triplicates, and data are derived from three independent experiments.

Real-time RT-PCR (qRT-PCR) assays

Total RNA was isolated from mouse DRG, human DRG and HEK-293 cells using Trizol Reagent (Invitrogen) and treated with RNase-free DNase I (Qiagen). 0.5-1μg total RNA was polyadenylated and reverse transcribed using Catch-All™ miRNA&mRNA RT-PCR Kit (Pengekiphen, Suzhou, China) according to the manufacturer's instructions. For detection of miRNA expression levels, qRT-PCR assays were conducted using the Catch-All™ miRNA&mRNA universal PCR primer as reverse primer, and the specific miRNA forward primers listed in Table S1[Sheet6]. The amplification conditions were an initial step at 95 °C for 10 min, followed by 40 cycles of 15 s at 95°C and 1 min at 60°C. All assays were performed in triplicate and included negative controls. The Ct value was recorded for each reaction, and the expression level of miRNA was calculated relative to *U6B*, a ubiquitously expressed snRNA, and *SHOX2* was normalized to either *Gapdh* or *18S RNA*. Data are presented as target gene expression = $2^{-\Delta ct}$.

***In ovo* electroporation**

pCAG-Shox2-IRES-GFP, *pCAG-miR-183-96-IRES-GFP* or backbone vector *pCAGIG* were injected into the neural tube of stage HH13 chicken embryos. Electroporation by five pulses of 40 V/cm was performed using a square wave electroporator (BTX). Embryos were harvested at E7.5 and fixed in 4% PFA/PBS for 6 hrs at 4 °C and sectioned at 14 μm thickness.

ACKNOWLEDGEMENTS

We thank Mr. Thomas Tingström for great help with taking care of all the mice. We also thank Sten Linnarsson group for providing assistance in RNA sequencing.

COMPETING INTERESTS

The authors declare no competing interests.

FUNDING

This work was supported by the Swedish Medical Research Council, Knut and Alice Wallenbergs Foundation (Wallenberg Scholar and Wallenberg project grant), Söderbergs Foundation, European Research Council (PainCells 740491) and Karolinska Institutet to (PE) and by the National Natural Science Foundation of China (Grant No.31741057) to Changgeng Peng. Human tissue retrieval was supported by CIMED.

DATA AVAILABILITY

All sequence data are available in GEO under the accession number GSE110714.

REFERENCES

Abdo, H., Li, L., Lallemend, F., Bachy, I., Xu, X. J., Rice, F. L. and Ernfors, P. (2011). Dependence on the transcription factor Shox2 for specification of sensory neurons conveying discriminative touch. *Eur J Neurosci* **34**, 1529-1541.

Abraira, V. E. and Ginty, D. D. (2013). The Sensory Neurons of Touch. *Neuron* **79**, 618-639.

Bak, M., Silahtaroglu, A., Moller, M., Christensen, M., Rath, M. F., Skryabin, B., Tommerup, N. and Kauppinen, S. (2008). MicroRNA expression in the adult mouse central nervous system. *Rna* **14**, 432-444.

Bernstein, E., Caudy, A. A., Hammond, S. M. and Hannon, G. J. (2001). Role for a bidentate ribonuclease in the initiation step of RNA interference. *Nature* **409**, 363-366.

Bernstein, E., Kim, S. Y., Carmell, M. A., Murchison, E. P., Alcorn, H., Li, M. Z., Mills, A. A., Elledge, S. J., Anderson, K. V. and Hannon, G. J. (2003). Dicer is essential for mouse development. *Nature genetics* **35**, 215-217.

Bourane, S., Garces, A., Venteo, S., Pattyn, A., Hubert, T., Fichard, A., Puech, S., Boukhaddaoui, H., Baudet, C., Takahashi, S., et al. (2009). Low-threshold mechanoreceptor subtypes selectively express MafA and are specified by Ret signaling. *Neuron* **64**, 857-870.

Busskamp, V., Krol, J., Nelidova, D., Daum, J., Szikra, T., Tsuda, B., Juttner, J., Farrow, K., Scherf, B. G., Alvarez, C. P., et al. (2014a). miRNAs 182 and 183 are necessary to maintain adult cone photoreceptor outer segments and visual function. *Neuron* **83**, 586-600.

Busskamp, V., Krol, J., Nelidova, D., Daum, J., Szikra, T., Tsuda, B., Juttner, J., Farrow, K., Scherf, B. G., Alvarez, C. P. P., et al. (2014b). MiRNAs 182 and 183 are necessary to maintain adult cone photoreceptor outer segments and visual function. *Hum Gene Ther* **25**, A23-A24.

Chalfie, M., Horvitz, H. R. and Sulston, J. E. (1981). Mutations that lead to reiterations in the cell lineages of C. elegans. *Cell* **24**, 59-69.

Cobb, J., Dierich, A., Huss-Garcia, Y. and Duboule, D. (2006). A mouse model for human short-stature syndromes identifies Shox2 as an upstream regulator of Runx2 during long-bone development. *Proceedings of the National Academy of Sciences of the United States of America* **103**, 4511-4515.

Dambal, S., Shah, M., Mihelich, B. and Nonn, L. (2015). The microRNA-183 cluster: the family that plays together stays together. *Nucleic acids research* **43**, 7173-7188.

Danielian, P. S., Muccino, D., Rowitch, D. H., Michael, S. K. and McMahon, A. P. (1998). Modification of gene activity in mouse embryos in utero by a tamoxifen-inducible form of Cre recombinase. *Curr Biol* **8**, 1323-1326.

Dykes, I. M., Lanier, J., Eng, S. R. and Turner, E. E. (2010). Brn3a regulates neuronal subtype specification in the trigeminal ganglion by promoting Runx expression during sensory differentiation. *Neural development* **5**, 3.

England, M. A. (1990). A color atlas of life before birth: Normal fetal development. *Wolfe Medical Publications, London*.

Fiorenza, A. and Barco, A. (2016). Role of Dicer and the miRNA system in neuronal plasticity and brain function. *Neurobiology of learning and memory*.

Gu, C., Li, X., Tan, Q., Wang, Z., Chen, L. and Liu, Y. (2013). MiR-183 family regulates chloride intracellular channel 5 expression in inner ear hair cells. *Toxicology in vitro : an international journal published in association with BIBRA* **27**, 486-491.

Honma, Y., Kawano, M., Kohsaka, S. and Ogawa, M. (2010). Axonal projections of mechanoreceptive dorsal root ganglion neurons depend on Ret. *Development* **137**, 2319-2328.

Islam, S., Zeisel, A., Joost, S., La Manno, G., Zajac, P., Kasper, M., Lonnerberg, P. and Linnarsson, S. (2014). Quantitative single-cell RNA-seq with unique molecular identifiers. *Nature methods* **11**, 163-166.

Karali, M., Peluso, I., Marigo, V. and Banfi, S. (2007). Identification and characterization of microRNAs expressed in the mouse eye. *Investigative ophthalmology & visual science* **48**, 509-515.

Kramer, I., Sigrist, M., de Nooij, J. C., Taniuchi, I., Jessell, T. M. and Arber, S. (2006). A role for Runx transcription factor signaling in dorsal root ganglion sensory neuron diversification. *Neuron* **49**, 379-393.

Lagos-Quintana, M., Rauhut, R., Meyer, J., Borkhardt, A. and Tuschl, T. (2003). New microRNAs from mouse and human. *Rna* **9**, 175-179.

Lallemend, F. and Ernfors, P. (2012). Molecular interactions underlying the specification of sensory neurons. *Trends in neurosciences* **35**, 373-381.

Langmead, B., Trapnell, C., Pop, M. and Salzberg, S. L. (2009). Ultrafast and memory-efficient alignment of short DNA sequences to the human genome. *Genome biology* **10**, R25.

Lecoin, L., Rocques, N., El-Yakoubi, W., Ben Achour, S., Larcher, M., Pouponnot, C. and Eychene, A. (2010). MafA transcription factor identifies the early ret-expressing sensory neurons. *Developmental neurobiology* **70**, 485-497.

Lee, R. C., Feinbaum, R. L. and Ambros, V. (1993). The C. elegans heterochronic gene lin-4 encodes small RNAs with antisense complementarity to lin-14. *Cell* **75**, 843-854.

Levanon, D., Bettoun, D., Harris-Cerruti, C., Woolf, E., Negreanu, V., Eilam, R., Bernstein, Y., Goldenberg, D., Xiao, C., Fliegauf, M., et al. (2002). The Runx3 transcription factor regulates development and survival of TrkC dorsal root ganglia neurons. *The EMBO journal* **21**, 3454-3463.

Lewis, M. A., Quint, E., Glazier, A. M., Fuchs, H., De Angelis, M. H., Langford, C., van Dongen, S., Abreu-Goodger, C., Piipari, M., Redshaw, N., et al. (2009). An ENU-induced mutation of miR-96 associated with progressive hearing loss in mice. *Nature genetics* **41**, 614-618.

Li, X., Kroin, J. S., Kc, R., Gibson, G., Chen, D., Corbett, G. T., Pahan, K., Fayyaz, S., Kim, J. S., van Wijnen, A. J., et al. (2013). Altered spinal microRNA-146a and the microRNA-183 cluster contribute to osteoarthritic pain in knee joints. *Journal of bone and mineral research : the official journal of the American Society for Bone and Mineral Research* **28**, 2512-2522.

Lin, C. R., Chen, K. H., Yang, C. H., Huang, H. W. and Sheen-Chen, S. M. (2014). Intrathecal miR-183 delivery suppresses mechanical allodynia in mononeuropathic rats. *The European journal of neuroscience* **39**, 1682-1689.

Liu, Y. and Ma, Q. (2011). Generation of somatic sensory neuron diversity and implications on sensory coding. *Current opinion in neurobiology* **21**, 52-60.

Lumayag, S., Haldin, C. E., Corbett, N. J., Wahlin, K. J., Cowan, C., Turturro, S., Larsen, P. E., Kovacs, B., Witmer, P. D., Valle, D., et al. (2013). Inactivation of the microRNA-183/96/182 cluster results in syndromic retinal degeneration. *Proceedings of the National Academy of Sciences of the United States of America* **110**, E507-516.

Luo, W., Enomoto, H., Rice, F. L., Milbrandt, J. and Ginty, D. D. (2009). Molecular identification of rapidly adapting mechanoreceptors and their developmental dependence on ret signaling.

Neuron **64**, 841-856.

Marmigere, F. and Ernfors, P. (2007). Specification and connectivity of neuronal subtypes in the sensory lineage. *Nature reviews. Neuroscience* **8**, 114-127.

Mencia, A., Modamio-Hoybjor, S., Redshaw, N., Morin, M., Mayo-Merino, F., Olavarrieta, L., Aguirre, L. A., del Castillo, I., Steel, K. P., Dalmay, T., et al. (2009). Mutations in the seed region of human miR-96 are responsible for nonsyndromic progressive hearing loss. *Nature genetics* **41**, 609-613.

Molliver, D. C., Wright, D. E., Leitner, M. L., Parsadanian, A. S., Doster, K., Wen, D., Yan, Q. and Snider, W. D. (1997). IB4-binding DRG neurons switch from NGF to GDNF dependence in early postnatal life. *Neuron* **19**, 849-861.

Peng, C., Li, L., Zhang, M. D., Bengtsson Gonzales, C., Parisien, M., Belfer, I., Usoskin, D., Abdo, H., Furlan, A., Haring, M., et al. (2017). miR-183 cluster scales mechanical pain sensitivity by regulating basal and neuropathic pain genes. *Science* **356**, 1168-1171.

Peng, C., Li, N., Ng, Y. K., Zhang, J., Meier, F., Theis, F. J., Merkenschlager, M., Chen, W., Wurst, W. and Prakash, N. (2012). A unilateral negative feedback loop between miR-200 microRNAs and Sox2/E2F3 controls neural progenitor cell-cycle exit and differentiation. *J Neurosci* **32**, 13292-13308.

Ryan, D. G., Oliveira-Fernandes, M. and Lavker, R. M. (2006). MicroRNAs of the mammalian eye display distinct and overlapping tissue specificity. *Molecular vision* **12**, 1175-1184.

Sacheli, R., Nguyen, L., Borgs, L., Vandenbosch, R., Bodson, M., Lefebvre, P. and Malgrange, B. (2009). Expression patterns of miR-96, miR-182 and miR-183 in the development inner ear. *Gene expression patterns : GEP* **9**, 364-370.

Scott, A., Hasegawa, H., Sakurai, K., Yaron, A., Cobb, J. and Wang, F. (2011). Transcription factor short stature homeobox 2 is required for proper development of tropomyosin-related kinase B-expressing mechanosensory neurons. *The Journal of neuroscience : the official journal of the Society for Neuroscience* **31**, 6741-6749.

Solda, G., Robusto, M., Primignani, P., Castorina, P., Benzoni, E., Cesarani, A., Ambrosetti, U., Asselta, R. and Duga, S. (2012). A novel mutation within the MIR96 gene causes non-syndromic inherited hearing loss in an Italian family by altering pre-miRNA processing. *Human molecular genetics* **21**, 577-585.

Usoskin, D., Furlan, A., Islam, S., Abdo, H., Lonnerberg, P., Lou, D., Hjerling-Leffler, J., Haeggstrom, J., Kharchenko, O., Kharchenko, P. V., et al. (2015). Unbiased classification of sensory neuron types by large-scale single-cell RNA sequencing. *Nat Neurosci* **18**, 145-153.

Wightman, B., Ha, I. and Ruvkun, G. (1993). Posttranscriptional regulation of the heterochronic gene lin-14 by lin-4 mediates temporal pattern formation in C. elegans. *Cell* **75**, 855-862.

Xu, S., Witmer, P. D., Lumayag, S., Kovacs, B. and Valle, D. (2007). MicroRNA (miRNA) transcriptome of mouse retina and identification of a sensory organ-specific miRNA cluster. *The Journal of biological chemistry* **282**, 25053-25066.

Yamada, S. and Takakuwa, T. (2012). Introduction - developmental overview of the human embryo. *In: S. Yamada (Ed), The Human Embryo, pp 3-20. InTech*.

Zehir, A., Hua, L. L., Maska, E. L., Morikawa, Y. and Cserjesi, P. (2010). Dicer is required for survival of differentiating neural crest cells. *Developmental biology* **340**, 459-467.

Zhang, H., Kolb, F. A., Jaskiewicz, L., Westhof, E. and Filipowicz, W. (2004). Single processing center models for human Dicer and bacterial RNase III. *Cell* **118**, 57-68.

Zhu, Q., Sun, W., Okano, K., Chen, Y., Zhang, N., Maeda, T. and Palczewski, K. (2011). Sponge transgenic mouse model reveals important roles for the microRNA-183 (miR-183)/96/182 cluster in postmitotic photoreceptors of the retina. *The Journal of biological chemistry* **286**, 31749-31760.

Figures

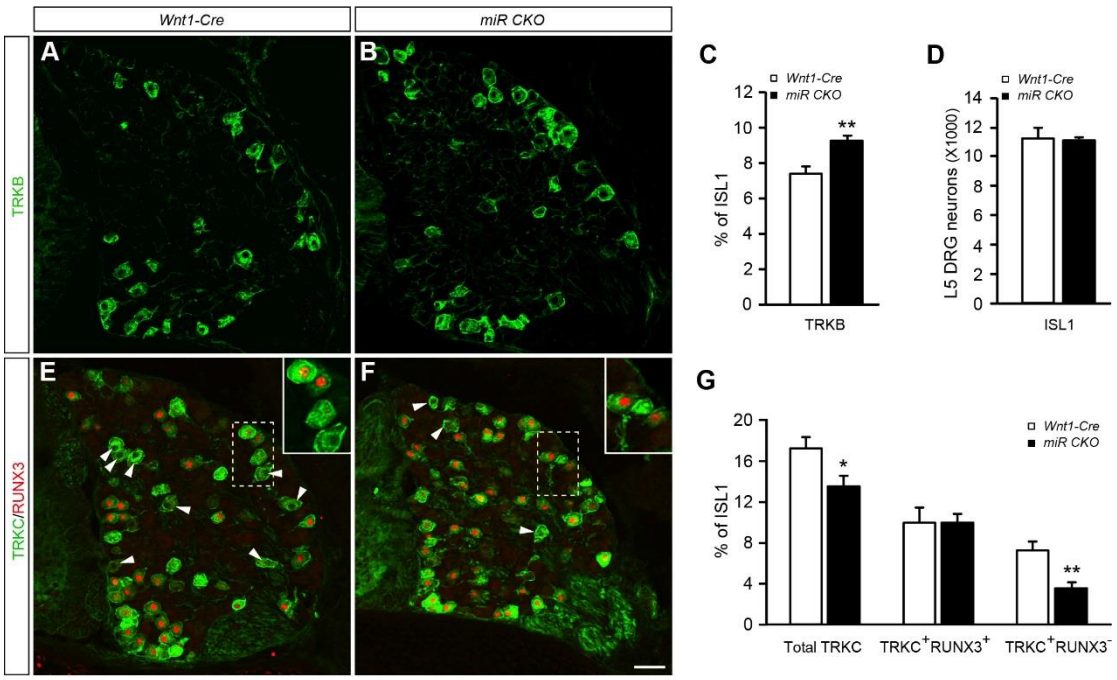

Fig. 1. The population sizes of TRKB$^+$ and TRKC$^+$ neurons are altered in the P0 *miR^{CKO}* mice.

(A-C) The percentage of TRKB$^+$ neurons was increased in the *miR^{CKO}* mice. Immunostaining for TRKB on DRG sections of control *Wnt1-Cre* mice (A) and the *miR^{CKO}* mice (B) as well as quantification of the percentage of TRKB$^+$ neurons in L3-L5 ganglions (C, n=3, 4).

(D) The number of total neurons (ISL1$^+$) in L5 DRG was not altered in the *miR^{CKO}* mice compared with controls (n=3, 4; not significant).

(E-G) The percent of total TRKC neurons were decreased in the *miR^{CKO}* mice. Double immunostaining for TRKC and RUNX3 on DRG sections of *Wnt1-Cre* mice (E) and *miR^{CKO}* mice (F), arrow heads in E and F point to NF3 (TRKC$^+$RUNX3$^-$) neurons, inset are higher magnifications of areas outlined in E and F. (G) Quantification of the percentage of total TRKC, TRKC$^+$RUNX3$^+$ (not significant) and TRKC$^+$RUNX3$^-$ neurons in L3-L5 ganglions (n=4, 4).

Data shown in mean±s.e.m. and analyzed by *t*-test and P<0.05 is statistically significant. *P<0.05, **P<0.01. Scale bar =50μM.

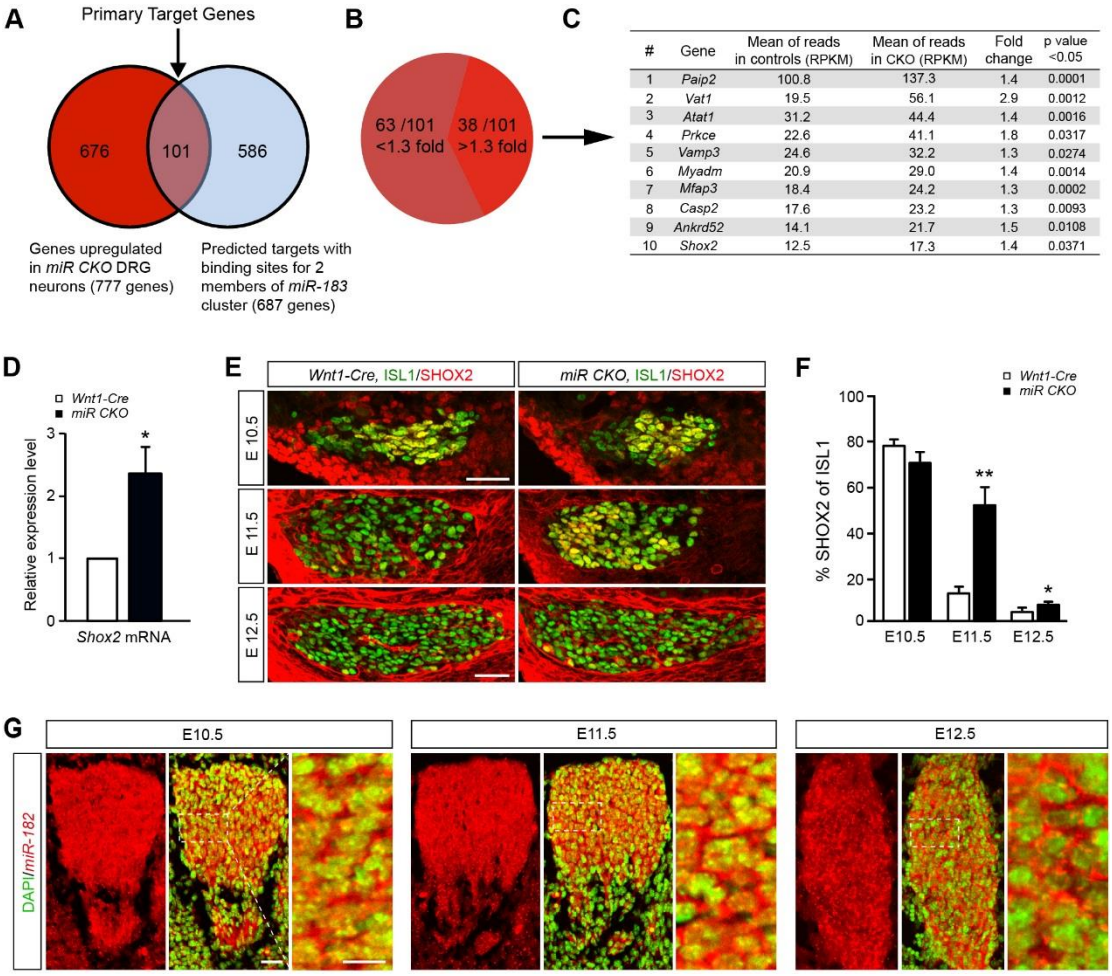

#	Gene	Mean of reads in controls (RPKM)	Mean of reads in CKO (RPKM)	Fold change	p value <0.05
1	*Paip2*	100.8	137.3	1.4	0.0001
2	*Vat1*	19.5	56.1	2.9	0.0012
3	*Atat1*	31.2	44.4	1.4	0.0016
4	*Prkce*	22.6	41.1	1.8	0.0317
5	*Vamp3*	24.6	32.2	1.3	0.0274
6	*Myadm*	20.9	29.0	1.4	0.0014
7	*Mfap3*	18.4	24.2	1.3	0.0002
8	*Casp2*	17.6	23.2	1.3	0.0093
9	*Ankrd52*	14.1	21.7	1.5	0.0108
10	*Shox2*	12.5	17.3	1.4	0.0371

Fig. 2. MiR-183 cluster terminates Shox2 expression in DRG neurons.

(A) Venn diagram shows the significantly upregulated (P<0.05) genes in the E12.5 miR^{CKO} mice from expression profiling data of DRG neurons (red) and TargetScan- predicted mRNA targets with binding sites for more than 1 members of miR-183 cluster (blue, Table S1[Sheet3]). The overlapping 101 genes were considered as potential targets of miR-183 cluster.

(B) Pie graph shows that 38 out of 101 target genes had greater than 1.3-fold increased mRNA expression and the remaining displayed less than 1.3 fold in miR^{CKO} mice.

(C) Shox2, a transcription factor playing a role in specification of DRG neurons, was among the top 10 high upregulated genes in miR^{CKO} mice.

(D) An increase of 2.3-fold *Shox2* mRNA level in the E12.5 miR^{CKO} mice was confirmed by real-time PCR, n=3, 3, data shown in mean±s.e.m. and analyzed by *t*-test, *P<0.05.

(E) SHOX2 is present in most E10.5 DRG neurons and is rapidly extinguished in most neurons at E11.5 in control mice but failed to be extinguished in miR^{CKO} mice.

(F) Quantification revealed that at E11.5 and E12.5 miR^{CKO} mice had more SHOX2 immunoreactive cells in the DRG than *Wnt1-Cre* controls, n=4, 4, *P<0.05, **P<0.01, by *t-test*.

(G) In situ hybridization for miR-182 at E10.5, E11.5 and E12.5 revealed that it is ubiquitously expressed in DRG neurons (DAPI, green).

Scale bar =50μM.

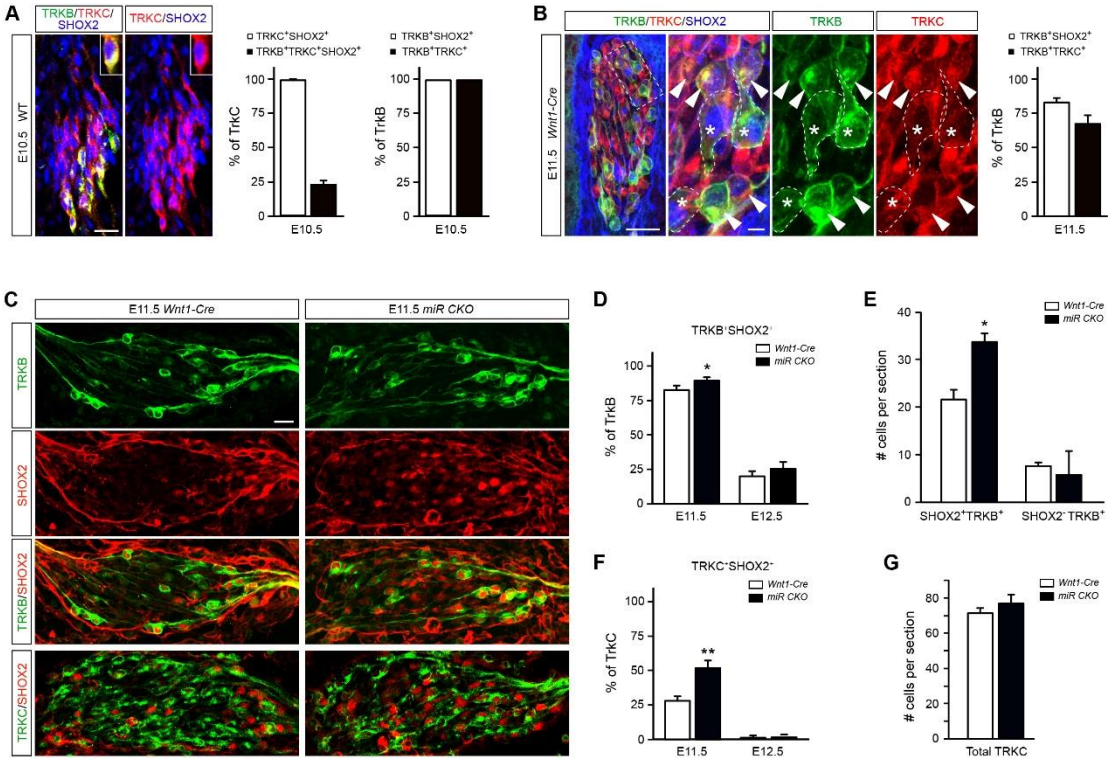

Fig. 3. SHOX2 expression fails to be extinguished in developing sensory neurons of *miR*^{CKO} mice.

(A) Immunostaining in wild-type mice for TRKB, TRKC and SHOX2 in E10.5 DRG and quantification to reveal the relation of SHOX2 expression to expression of TRKB and TRKC (n=4). Scale bar = 50 μm.

(B) Immunostaining in wild-type mice for TRKB, TRKC and SHOX2 in E11.5 DRG and quantification to reveal the relation of SHOX2 expression to expression of TRKB and TRKC. Many SHOX2^{+}/TRKB^{+} neurons lost membrane TRKC^{+} staining, indicating its down-regulation (asterisks) while neurons with membrane TRKC staining rarely contained SHOX2 (arrow heads). Quantification is of all positive cells (n=4). Scale bar = 50 μm and 10 μm in the enlarged inset.

(C) Double immunostaining for TRKB/SHOX2 or TRKC/SHOX2 on DRG sections of *Wnt1-Cre* and the *miR*^{CKO} mice. Scale bar = 50 μm.

(D) Quantification of the percent of TRKB^{+}/SHOX2^{+} neurons to all TRKB neurons in the DRG of E11.5 *Wnt1-Cre* control mice and *miR*^{CKO} mice (n=4,4), *P<0.05 by Student t test.

(E) Quantification of the number of SHOX2^{+}/TRKB^{+} and SHOX2^{-}/TRKB^{+} neurons revealed an increased number of SHOX2^{+}/TRKB^{+} DRG neurons in *miR*^{CKO} compared to *Wnt1-Cre* control mice at E11.5 (n=4,4), *P<0.05 by Student t test.

(F) Quantification of the percent of TRKC^{+}/SHOX2^{+} neurons to all TRKC neurons in the DRG of E11.5 *Wnt1-Cre* control mice and *miR*^{CKO} mice (n=4,4), **P<0.01 by Student t test.

(G) Quantification of the number of TRKC^{+} neurons in DRG of *Wnt1-Cre* control mice and *miR*^{CKO} mice (n=4,4).

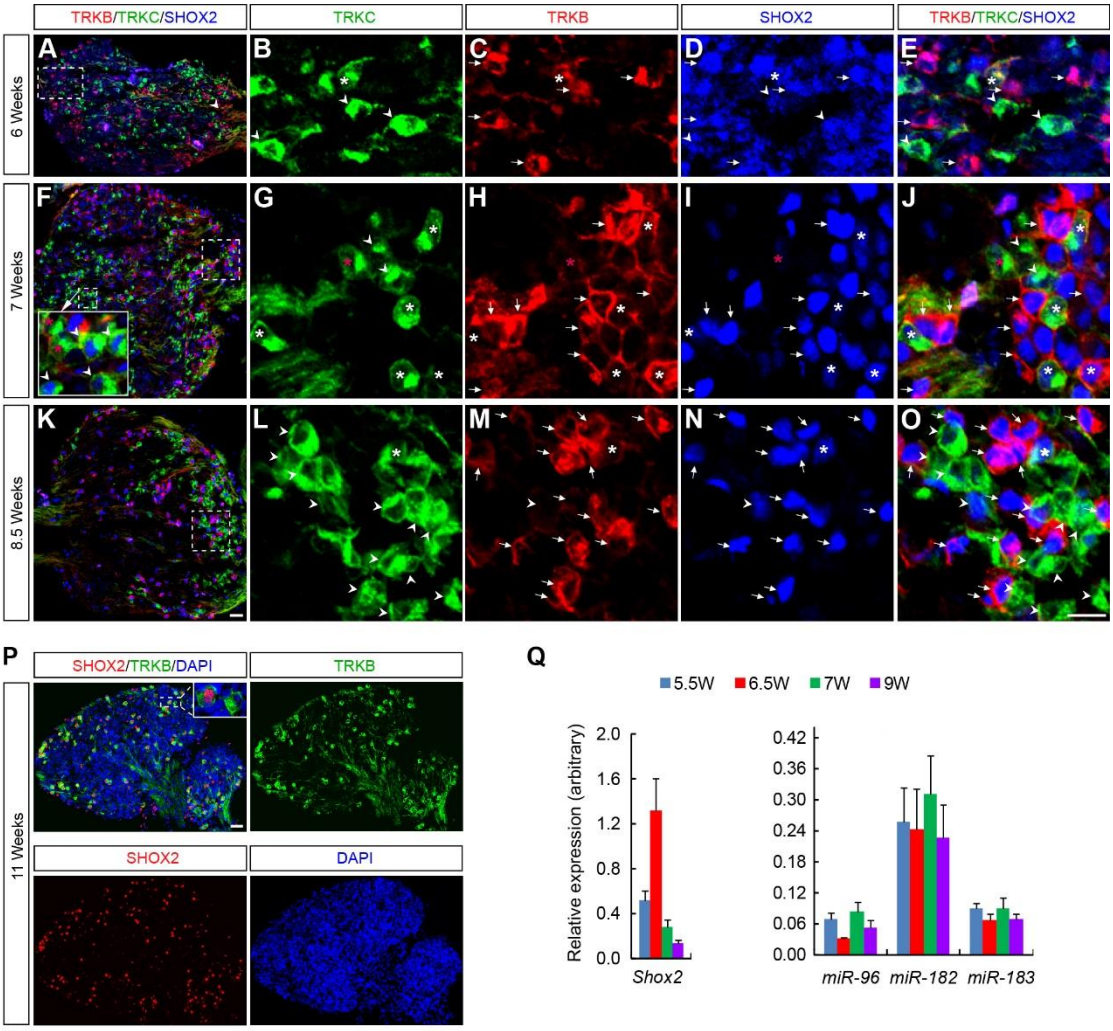

Fig. 4. Expression of miR-183 cluster and SHOX2 in the developing human DRG.

(A-O) Expression of SHOX2 overlapped with TRKB and/or TRKC expression in week 6 and week 7 DRG but very rarely co-exists with TRKC at week 8.5. Triple immunostaining for TRKB (red), TRKC (green) and SHOX2 (blue) on DRG section of 6-8.5 weeks human embryos shows that SHOX2 was weakly expressed in DRG and some TRKB neurons co-express TRKC at week 6 (A-E, B-E are zoom in view of area outlined in A). SHOX2 expression was present in TRKB and/or TRKC neurons at week 7 (F-J, G-J are zoom in view of area outlined in F), however, at 8.5 weeks SHOX2 were maintained in $TRKB^+$ neurons while most of TRKC neurons lost SHOX2 (K-O, L-O are zoom in view of area outlined in K). Arrow head points to $TRKC^+$ neurons, arrow points to $TRKB^+$ neurons and white asterisk mark $TRKB^+/TRKC^+/SHOX2^+$ neurons, respectively. Scale bar =50μM.

(P) In the 11 weeks old human embryo, SHOX2 is extinguished in all but $TRKB^+$ neurons. Scale bar =50μM.

(Q) Detection of *Shox2* and *miR-183-96-182* expression level in DRG from 5.5 to 9 weeks human embryos by qPCR. The expression level of *Shox2* and *miR-183-96-182* were normalized to internal control 18S RNA and U6B, respectively (data shown in mean±s.e.m.value of three technical repeats).

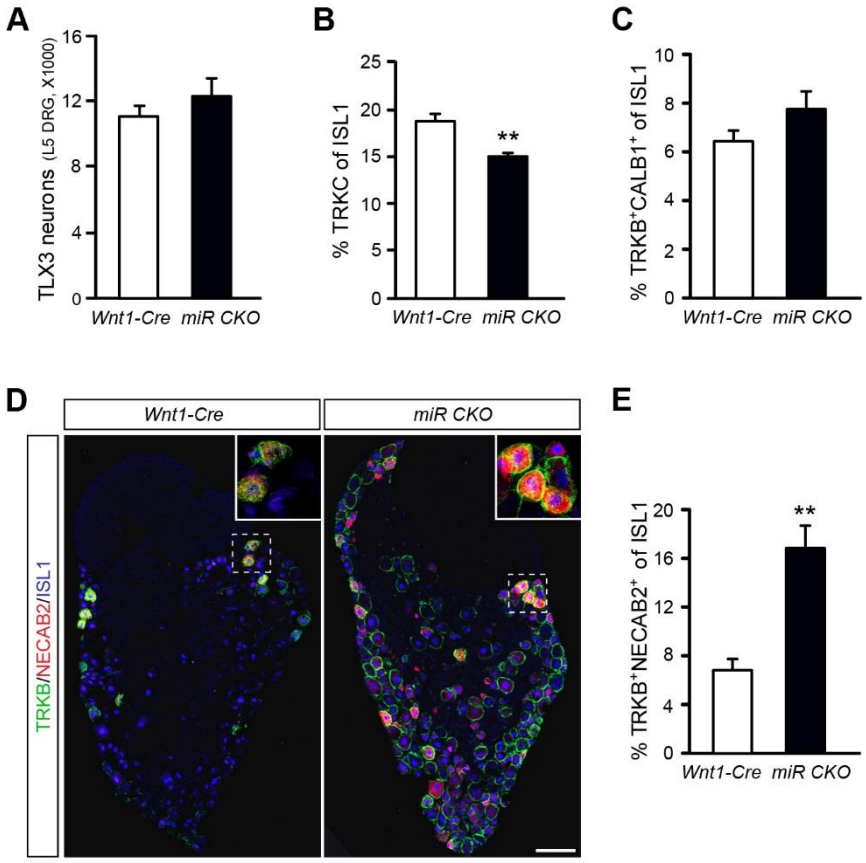

Fig. 5. MiR-183 cluster determines the adult proportion of Aδ LTMRs and Aβ SA-LTMRs but not Aβ RA-LTMRs.

(A) Quantification of L5 DRG shows that there was no difference in the total number of neurons between the *miR*^{CKO} mice and age-matched *Wnt1-Cre* control mice, (n=3, 3, P=0.376).

(B) The percentage of TRKC^{+} neurons was decreased in the *miR*^{CKO} mice when compared to control mice, (n=3, 3, **P<0.01).

(C) The percentage of TRKB^{+}/CALB1^{+} neurons was not significantly changed in the *miR*^{CKO} mice (n=3, 3, P=0.227).

(D, E) The percentage of TRKB^{+}/ NECAB2^{+} neurons was increased in the *miR*^{CKO} mice. (D) Triple immunostaining for TRKB (green), NECAB2 (red) and ISL1 (blue) on DRG sections. (E) **Quantification in the *miR*^{CKO} mice compared to *Wnt1-Cre*. (n=3, 3, **P<0.01). Data shown in mean±s.e.**m. and analyzed by *t*-test. Scale bar =50μM.

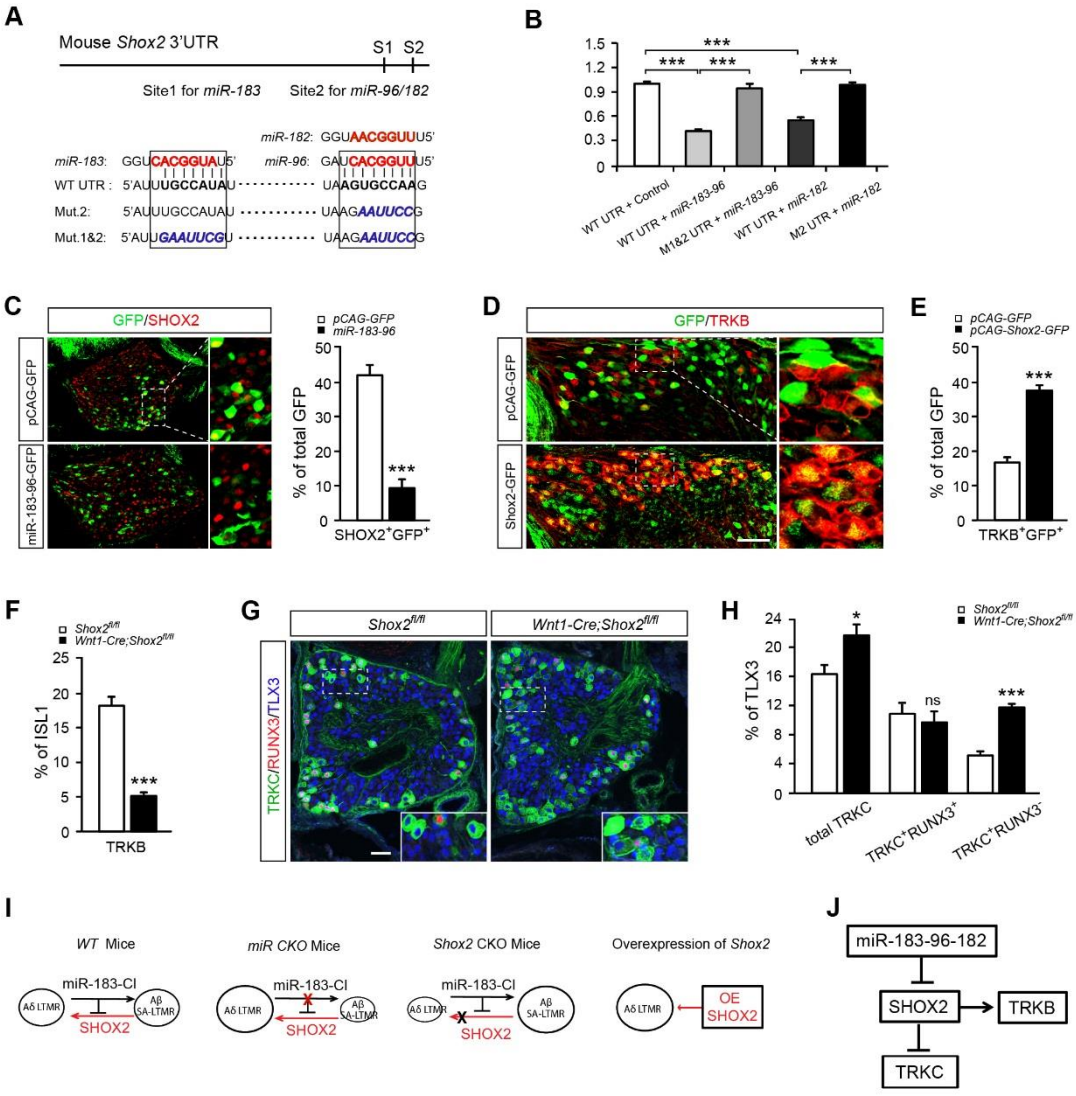

Fig. 6. MiR-183 cluster directly regulates Shox2 to affect the proportions of subgroup neurons in DRG

(A) Schematic illustration of the mouse *Shox2* UTR with two putative binding sites (S1, S2) for miR-183 cluster. The seed sequence of microRNA is in red bold letters, the binding sequence of the seed sequence is in black bold letters and the mutated binding site sequence is in blue Italic letters. The binding site 1 on Shox2 UTR has 7 nucleotides which match to miR-183, and the binding site 2 has 8 and 7 nucleotides which match to miR-96 and miR-182 respectively.

(B) miR-183 cluster repressed *Shox2* expression via binding onto its UTR. Co-transfection of *miR-183-96* into HEK293 cells can repress the expression of the *firefly luciferase* gene which bears a fragment covering S1 and S2 of Shox2 UTR (grey bar) when compared to empty vector-co-transfected control (white bar). This repression was completely abolished when both binding sites S1 and S2 were mutated (dark bar). miR-182 can also repress the expression of the *firefly luciferase* gene which bears a fragment covering S1 and S2 of Shox2 UTR (blue bar) when compared to empty vector-co-transfected control (white bar), and the repression was absent when site 2 was mutated (pink bar). ***P≤0.001. M1&2 stands for mutation on both site 1 and 2, M2 stands mutation on site 2. See Fig. S4 for detailed information about the used plasmids. Data

shown in mean±s.d. from four independent experiments with triplicates per assay.

(C) Forced expression of *miR-183-96* can repress endogenous SHOX2 expression *in vivo*. Electroporation of *pCAG-miR-183-96-IRES-GFP* plasmid into neural crest cells of stage HH13 chicken embryo and analysis at E7.5. Immunostaining for SHOX2 (red) and GFP (green) on DRG section demonstrated that miR-183-96 dramatically repressed endogenous expression of SHOX2 *in vivo* when compared to *pCAG-IRES-GFP*-electroporated control (n=4, 3, ***P=0.001). Scale bar =50μM.

(D-E) Overexpression of Shox2 caused an increase of $TRKB^+$ neurons in chicken DRG. Electroporation of pCAG-Shox2 -IRES-GFP plasmid into neural crest cells of HH13 chicken embryos, which were subsequently harvested at E7.5 and then immunostaining for TRKB (red) and GFP (green) on DRG section shows that overexpression of Shox2 resulted in an increase of $TRKB^+$ neurons when compared to pCAG-IRES-GFP-electroporated control (n=4, 4, ***P<0.0001).

(F) Loss of Shox2 led to a decrease in the proportion of TRKB neurons in the *Wnt-1-Cre; Shox2* $^{fl/fl}$ mice when compared to *Shox2* $^{fl/fl}$ controls (n=3, 4, ***P<0.001).

(G-H) Immunostaining for TRKC (green), RUNX3 (red) and TLX3 (blue) shows that the proportions of TRKC (n=3, 3, *P<0.05) and $TRKC^+/RUNX3^-$ (n=3, 3, ***P<0.001) neurons in the P0 *Wnt-1-Cre; Shox2* $^{fl/fl}$ mice were increased, but not $TRKC^+/RUNX3^+$ (n=3, 3, P=0.6).

(I) Summary of phenotypes observed in the different animal experiments. Aδ LTMR ($TRKB^+/NECAB2^+$) and Aβ SA-LTMRs ($TRKC^+/RUNX3^-$) refer to the lineage of these types of LTMRs based on marker expression during development. Abbreviations: miR-183-Cl, miR-183 cluster; OE, overexpression; miR CKO mice, *Wnt1-Cre; miR-183-96-182* $^{flox/flox}$, *Shox2* CKO mice, *Wnt1-Cre; Shox2* $^{flox/flox}$.

(J) Gene-regulatory network proposed to regulate Aδ LTMR and Aβ SA-LTMRs.

Except panel B, all other data shown in mean±s.e.m. and analyzed by *t*-test, Scale bar =50μM.

Supplementary Figures

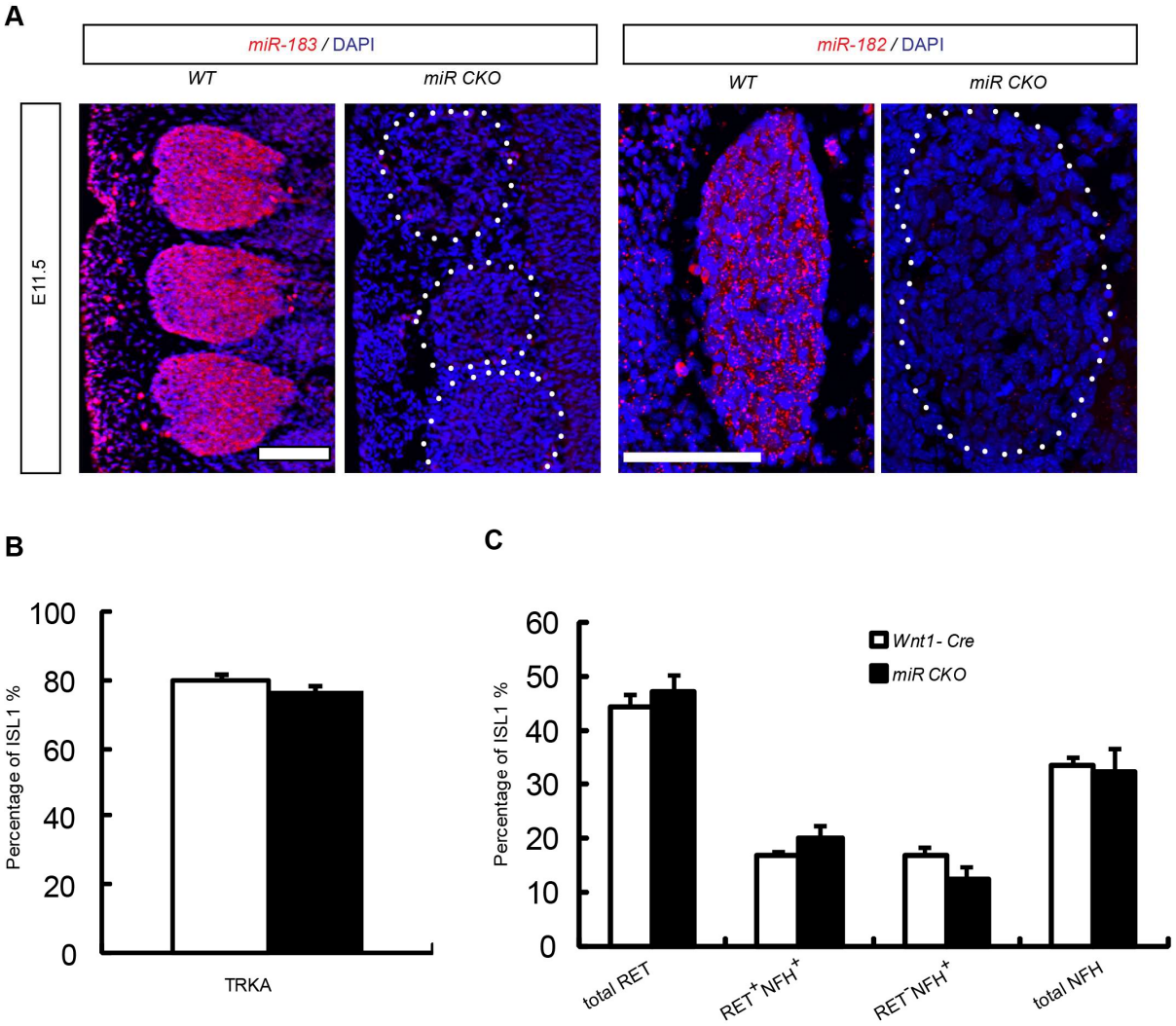

Fig. S1 (Related to Fig.1). Depletion of miR-183 cluster in the *miR*^{CKO} mice and the numbers of TRKA, RET and NFH DRG neurons were not changed in P0 *miR*^{CKO} mice compared to *Wnt1-cre* control mice.

(A) Expression of miR-183 cluster was depleted in the *miR*^{CKO} mice. Images were collected from E11.5 mouse embryos. DRG are circled by dashed line. Scale bar =100μM.

(B) Quantification of the expressing neurons as percent of all neurons (n=5, 4; P=0.23), in L3-L5 ganglia.

(C) Quantification of RET and NFH expressing neurons as percent of all neurons (n=3, 3, p>0.05), in L3-L5 ganglia.

Data shown as mean±s.e.m. and analyzed by t-test.

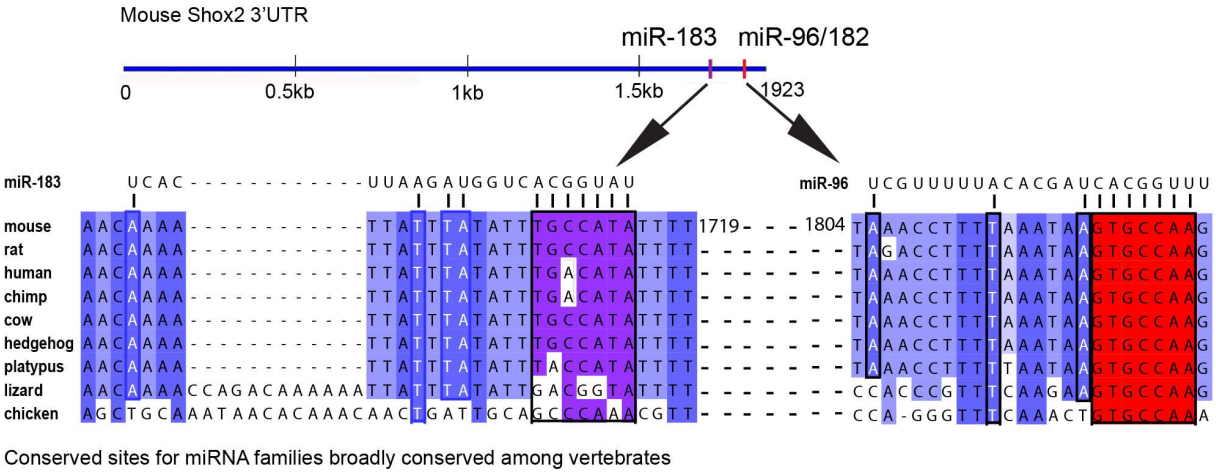

Fig. S2 (Related to Fig.2). Shox2 is a putative conserved target of miR-183 cluster.

Schematic illustration for mouse Shox2 3'UTR carrying two binding sites for miR-183 cluster predicted by TargetScan algorithm (upper panel). These two binding sites are highly conserved among more than 12 species and the sequences matching to the seed sequence of miR-183 and miR-96 are marked in purple or red (Bottom panel). The binding site for miR-96/182 perfectly matches all 7-nucleotides of miR-96's seed sequence and matches 6-nucleotides of miR-182's seed sequence; and this 7-nucleotides sequence is conserved in vertebrates from lizard to human. Due to that chick *Shox2* 3'UTR has not been annotated, TargetScan did not identify any target site for miR-96/182. Nevertheless, as a target site was discovered by TargetScan in lizard, a lower species in the evolutionary tree, so we therefore predicted that it is probably also presented in chicken. We therefore extracted the sequence of chick Shox2 3'UTR from ENSEMBL database and indeed found that the binding site for miR-96 is also conserved on chick Shox2 3'UTR. However, the miR-183 binding site is not as conserved in chicken as the miR-96/182 cluster.

Methods for Fig. S2:

The sequence alignment is based on the alignment from the microRNA prediction server Target Scan Human (Release 6.2) for the Shox2 mouse UTR. All sequences were extracted from ENSEMBL database (release 77，(Flicek et al., 2014)). For the multiple sequence alignment of the orthologs the following parts of the 3´UTR or 3´ flanking sequences of the Shox2 gene were used:

Mouse (*Mus musculus*): ENSMUST00000162098 utr3: bp 1600-1923; Rat (*Rattus norvegicus*): 3' Flanking sequence chromosome:Rnor_5.0:2:183467529:183467829:-1; Human (*Homo sapiens*): ENST00000441443 utr3: bp1700-2016; Chimpanzee (*Pan troglodytes*): 3' Flanking sequence chromosome: CHIMP2.1.4:3:161850370:161850670:-1; Cow (*Bos taurus*): 3' Flanking sequence chromosome: UMD3.1:1:110287694:110287994:1; Hedgehog (*Erinaceus europaeus*): 3' Flanking sequence scaffold: HEDGEHOG:scaffold_376919:35520:35820:-1; Platypus (*Ornithorhynchus anatinus*): 3' Flanking sequence supercontig: OANA5:Contig3858:24433:24733:1; Anole Lizard (*Anolis carolinensis*): 3' Flanking sequence chromosome:AnoCar2.0:3:14459478:14460078:1; Chicken (*Gallus gallus*): 3' Flanking sequence chromosome: Galgal4:9: for predicted miR183 binding: 22087348:22087948:1

The multiple sequence alignment was performed with the ClustalW2 (Larkin et al., 2007) web server and visualized by using the Jalview software (Waterhouse et al., 2009).

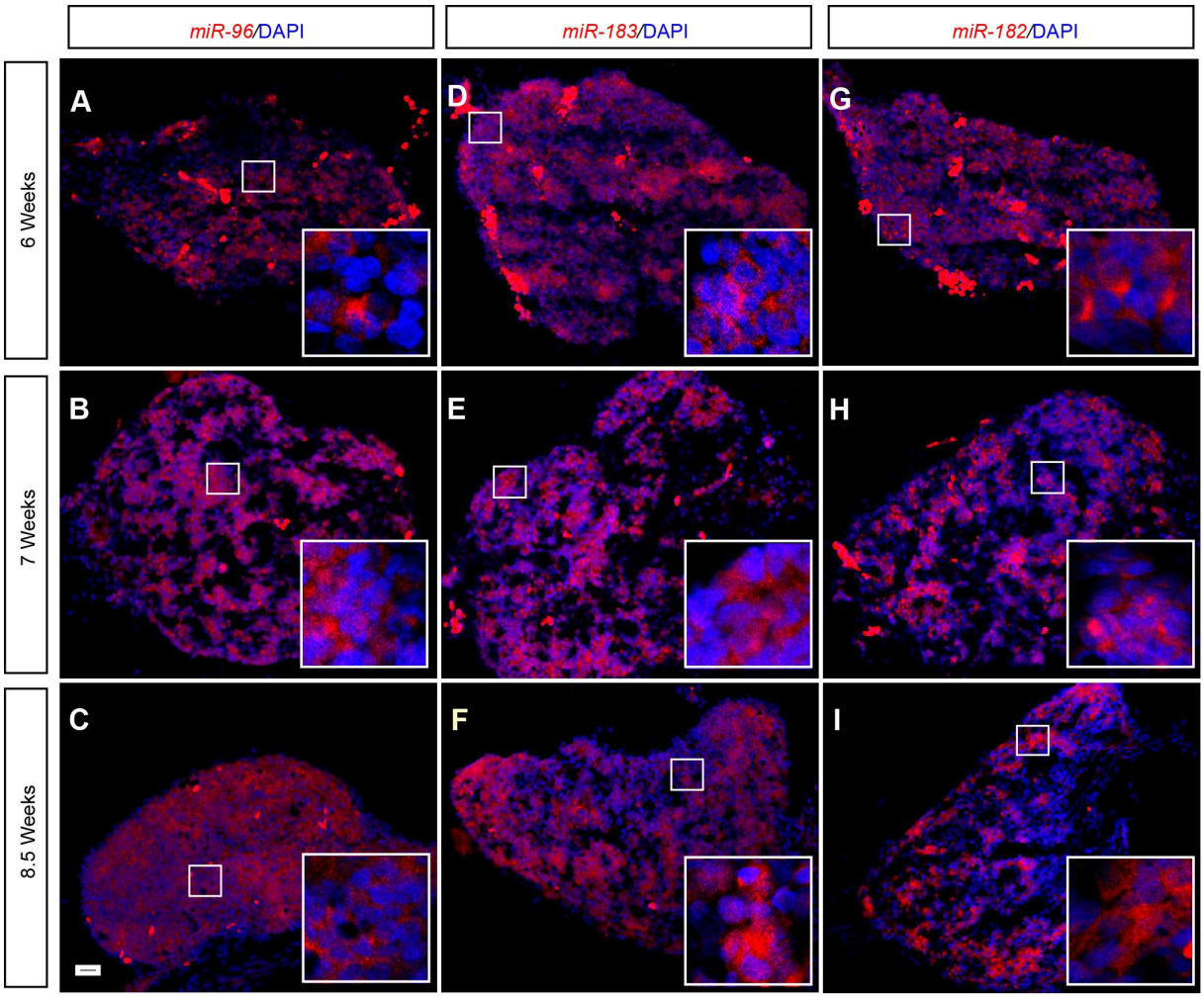

Fig. S3 (Related to Fig.4). Expression of miR-183 cluster in the embryonic human DRG.

In situ hybridization for miR-96 (A-C), miR-183 (D-F) and miR-183 (G-I) shows that miR-183 cluster is broadly expressed in human DRG at 6 weeks (A, D, G), 7 weeks (B, E, K), 8.5 weeks (C, F, I). Scale bar =50μM.

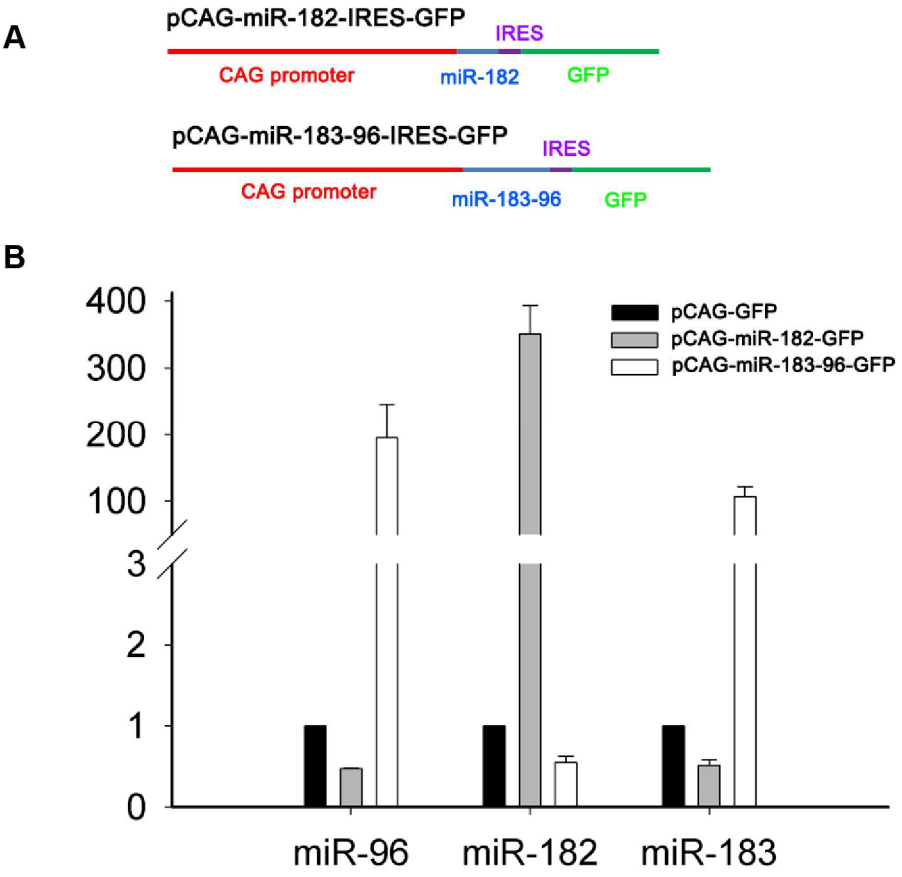

Fig. S4 (Related to Fig.6). Overexpression vectors for miR-182 and miR-183-96 as well as their overexpression level in HEK293 cells after transfection.

(A) Schematic maps of pCAG-miR-182-IRES-GFP and pCAG -miR-183-96-IRES-GFP vectors.

(B) qPCR demonstrated that pCAG-miR-182-IRES-GFP-transfected HEK293 cells had increased expression level of miR-182 (3 bars in middle) compared to the pCAG-GFP-transfected HEK293 cells, and that pCAG-miR-183-96-IRES-GFP-transfected HEK293 cells had increased expression level of both miR-183 (3 bars in right) and miR-96 (3 bars in left) compared to the pCAG-GFP-transfected HEK293 cells. Expression is presented in arbitrary units where control vector is set at 1. Data shown as mean±s.e.m. from three independent experiments.

Supplementary Table

Table S1^{sheet1}. RNA-seq data (Reads Per Kilobase Million, RPKM) from E12.5 DRG of 3 Controls（2 *Wnt1-Cre* and 1 *WT*） and 3 *Wnt1-Cre; miR$^{fl/fl}$* mice.

Table S1^{sheet2}. Significantly upregulated genes (P<0.05) in DRG of the *miR^{CKO}* mice.

Table S1^{sheet3}. TargetScan algorithm predicted genes targeted by more than one member of miR-183 cluster.

Table S1^{sheet4}. Total 38 genes carrying binding sites of more than one members of miR-183 cluster and upregulated ⩾1.3 fold. Among these, two were transcription factors which are marked in red (Shox2 and Zbtb41).

Table S1^{sheet5}. The sequences synthesized and cloned in vectors for overexpression of miR-183-96 and miR-182. Underlined are the precursor sequences for each miRNA.

Table S1^{sheet6}. The list of primers used for cloning mouse *Shox2* 3'UTR for luciferase assay and primers for qRT-PCR.

Click here to Download Table S1

Supplementary Reference

Flicek, P., Amode, M. R., Barrell, D., Beal, K., Billis, K., Brent, S., Carvalho-Silva, D., Clapham, P., Coates, G., Fitzgerald, S., et al. (2014). Ensembl 2014. *Nucleic Acids Res* **42**, D749-755.

Larkin, M. A., Blackshields, G., Brown, N. P., Chenna, R., McGettigan, P. A., McWilliam, H., Valentin, F., Wallace, I. M., Wilm, A., Lopez, R., et al. (2007). Clustal W and Clustal X version 2.0. *Bioinformatics* **23**, 2947-2948.

Waterhouse, A. M., Procter, J. B., Martin, D. M., Clamp, M. and Barton, G. J. (2009). Jalview Version 2--a multiple sequence alignment editor and analysis workbench. *Bioinformatics* **25**, 1189-1191.

Supplementary Figures

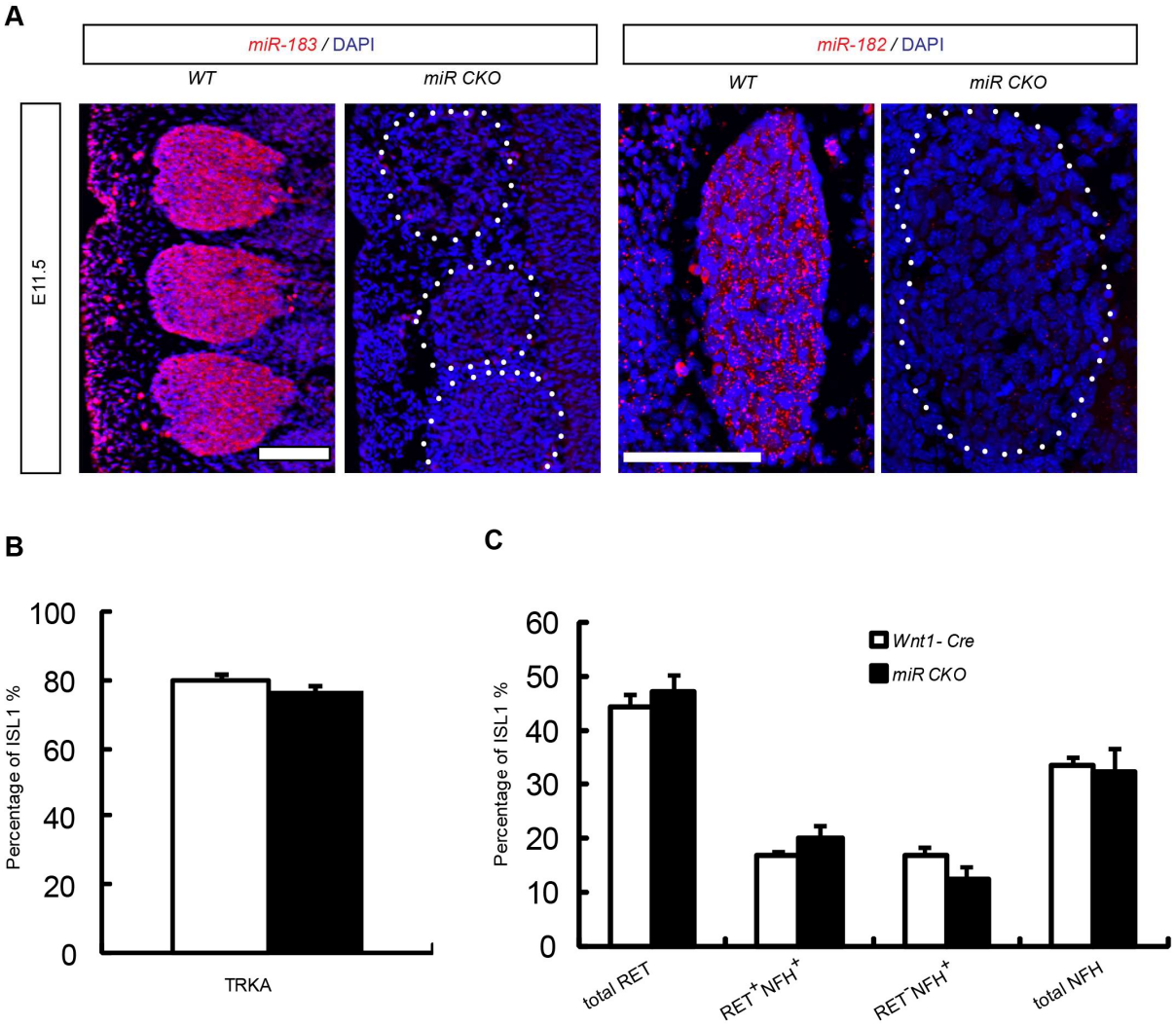

Fig. S1 (Related to Fig.1). Depletion of miR-183 cluster in the *miR*^{CKO} mice and the numbers of TRKA, RET and NFH DRG neurons were not changed in P0 *miR*^{CKO} mice compared to *Wnt1-cre* control mice.

(A) Expression of miR-183 cluster was depleted in the *miR*^{CKO} mice. Images were collected from E11.5 mouse embryos. DRG are circled by dashed line. Scale bar =100μM.

(B) Quantification of the expressing neurons as percent of all neurons (n=5, 4; P=0.23), in L3-L5 ganglia.

(C) Quantification of RET and NFH expressing neurons as percent of all neurons (n=3, 3, p>0.05), in L3-L5 ganglia.

Data shown as mean±s.e.m. and analyzed by t-test.

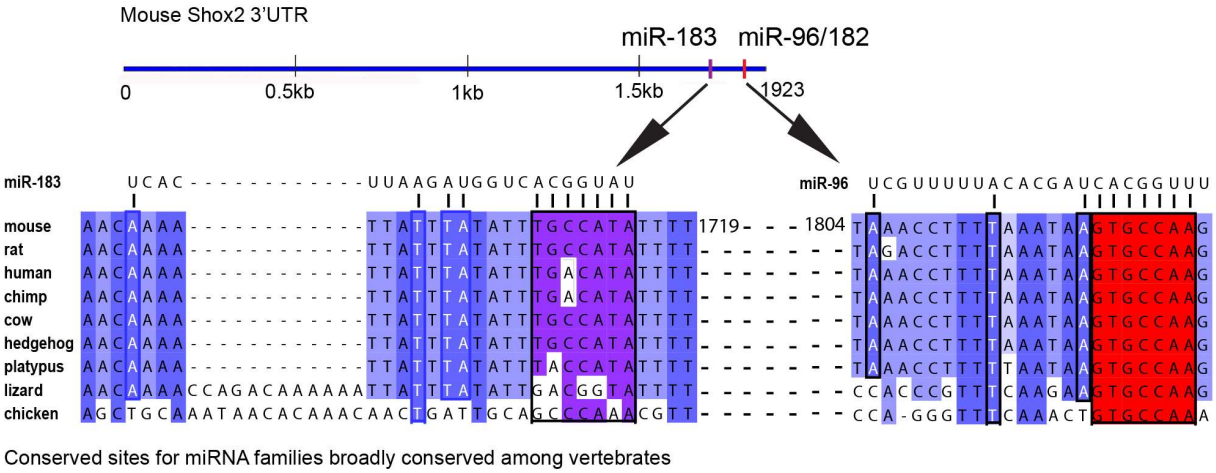

Fig. S2 (Related to Fig.2). Shox2 is a putative conserved target of miR-183 cluster.

Schematic illustration for mouse Shox2 3'UTR carrying two binding sites for miR-183 cluster predicted by TargetScan algorithm (upper panel). These two binding sites are highly conserved among more than 12 species and the sequences matching to the seed sequence of miR-183 and miR-96 are marked in purple or red (Bottom panel). The binding site for miR-96/182 perfectly matches all 7-nucleotides of miR-96's seed sequence and matches 6-nucleotides of miR-182's seed sequence; and this 7-nucleotides sequence is conserved in vertebrates from lizard to human. Due to that chick *Shox2* 3'UTR has not been annotated, TargetScan did not identify any target site for miR-96/182. Nevertheless, as a target site was discovered by TargetScan in lizard, a lower species in the evolutionary tree, so we therefore predicted that it is probably also presented in chicken. We therefore extracted the sequence of chick Shox2 3'UTR from ENSEMBL database and indeed found that the binding site for miR-96 is also conserved on chick Shox2 3'UTR. However, the miR-183 binding site is not as conserved in chicken as the miR-96/182 cluster.

Methods for Fig. S2:

The sequence alignment is based on the alignment from the microRNA prediction server Target Scan Human (Release 6.2) for the Shox2 mouse UTR. All sequences were extracted from ENSEMBL database (release 77，(Flicek et al., 2014)). For the multiple sequence alignment of the orthologs the following parts of the 3´UTR or 3´ flanking sequences of the Shox2 gene were used:

Mouse (*Mus musculus*): ENSMUST00000162098 utr3: bp 1600-1923; Rat (*Rattus norvegicus*): 3' Flanking sequence chromosome:Rnor_5.0:2:183467529:183467829:-1; Human (*Homo sapiens*): ENST00000441443 utr3: bp1700-2016; Chimpanzee (*Pan troglodytes*): 3' Flanking sequence chromosome: CHIMP2.1.4:3:161850370:161850670:-1; Cow (*Bos taurus*): 3' Flanking sequence chromosome: UMD3.1:1:110287694:110287994:1; Hedgehog (*Erinaceus europaeus*): 3' Flanking sequence scaffold: HEDGEHOG:scaffold_376919:35520:35820:-1; Platypus (*Ornithorhynchus anatinus*): 3' Flanking sequence supercontig: OANA5:Contig3858:24433:24733:1; Anole Lizard (*Anolis carolinensis*): 3' Flanking sequence chromosome:AnoCar2.0:3:14459478:14460078:1; Chicken (*Gallus gallus*): 3' Flanking sequence chromosome: Galgal4:9: for predicted miR183 binding: 22087348:22087948:1

The multiple sequence alignment was performed with the ClustalW2 (Larkin et al., 2007) web server and visualized by using the Jalview software (Waterhouse et al., 2009).

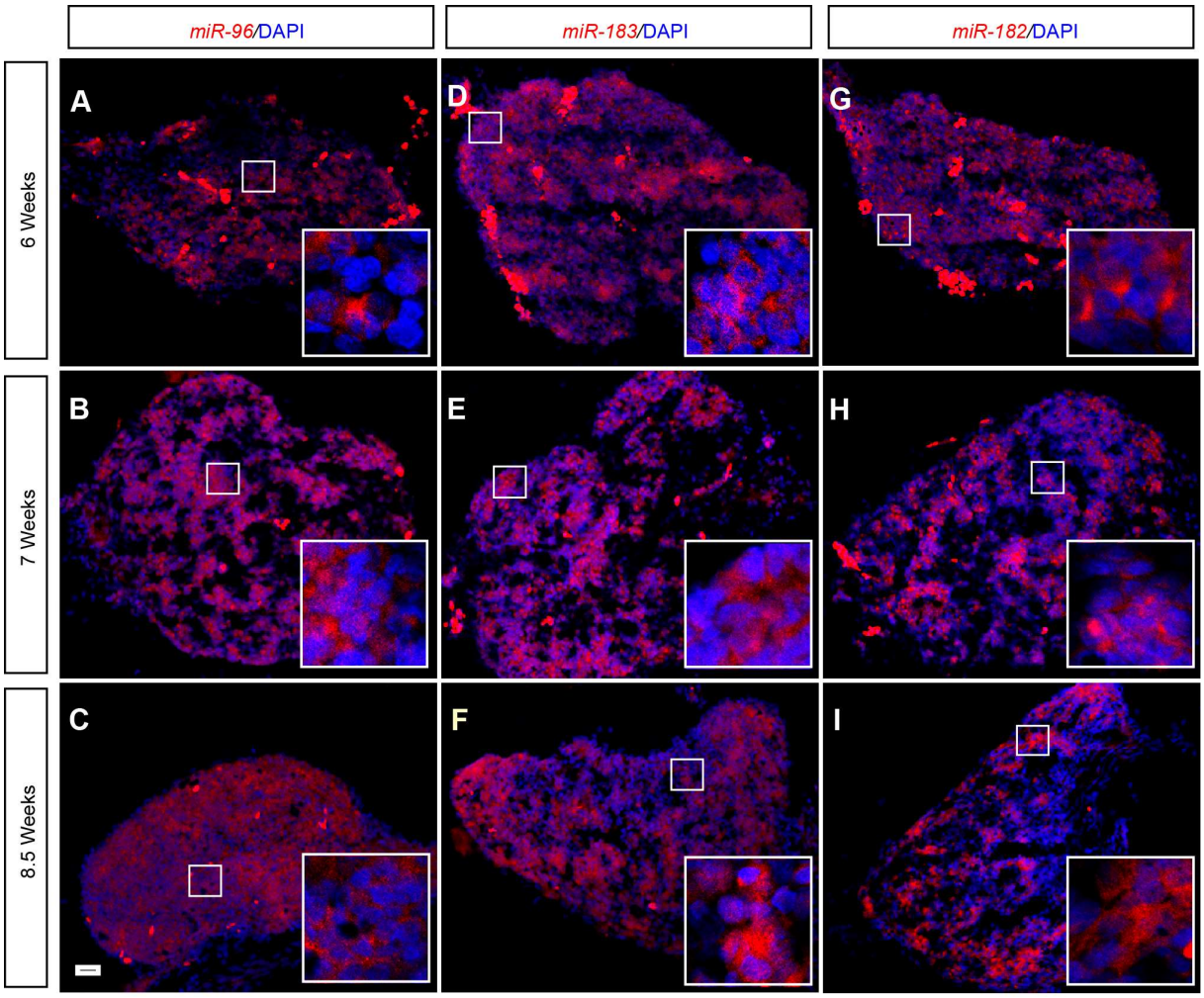

Fig. S3 (Related to Fig.4). Expression of miR-183 cluster in the embryonic human DRG.

In situ hybridization for miR-96 (A-C), miR-183 (D-F) and miR-183 (G-I) shows that miR-183 cluster is broadly expressed in human DRG at 6 weeks (A, D, G), 7 weeks (B, E, K), 8.5 weeks (C, F, I). Scale bar =50μM.

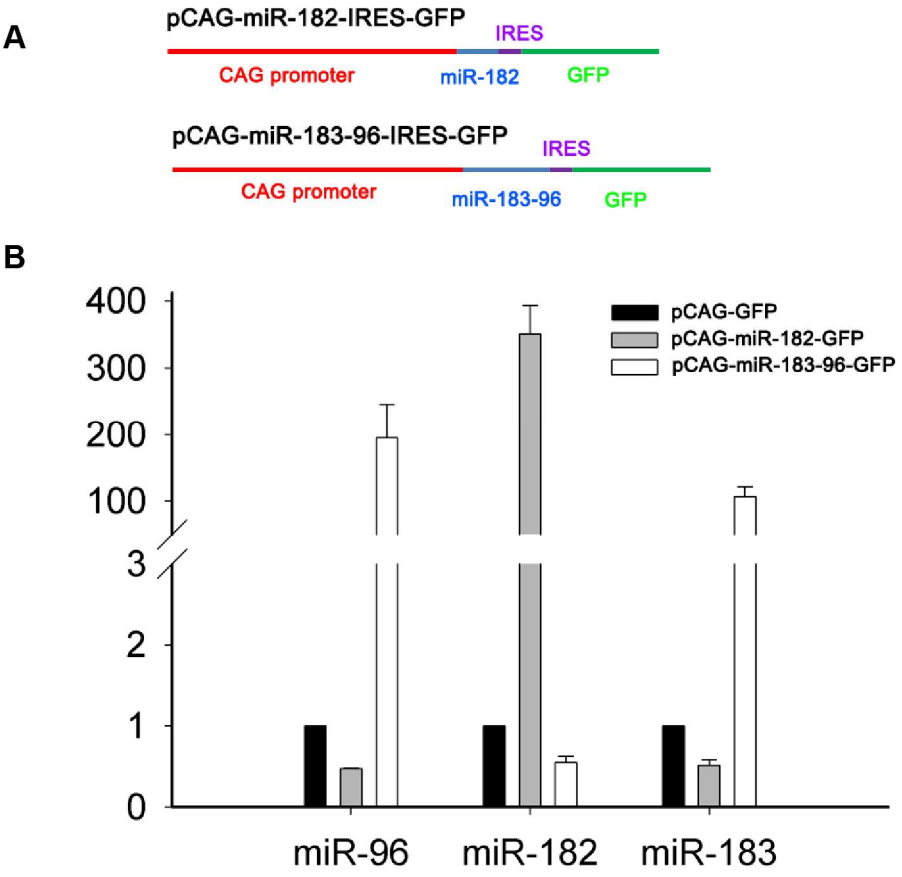

Fig. S4 (Related to Fig.6). Overexpression vectors for miR-182 and miR-183-96 as well as their overexpression level in HEK293 cells after transfection.

(A) Schematic maps of pCAG-miR-182-IRES-GFP and pCAG -miR-183-96-IRES-GFP vectors.

(B) qPCR demonstrated that pCAG-miR-182-IRES-GFP-transfected HEK293 cells had increased expression level of miR-182 (3 bars in middle) compared to the pCAG-GFP-transfected HEK293 cells, and that pCAG-miR-183-96-IRES-GFP-transfected HEK293 cells had increased expression level of both miR-183 (3 bars in right) and miR-96 (3 bars in left) compared to the pCAG-GFP-transfected HEK293 cells. Expression is presented in arbitrary units where control vector is set at 1. Data shown as mean±s.e.m. from three independent experiments.

Supplementary Table

Table S1^{sheet1}. RNA-seq data (Reads Per Kilobase Million, RPKM) from E12.5 DRG of 3 Controls（2 *Wnt1-Cre* and 1 *WT*） and 3 *Wnt1-Cre; miR$^{fl/fl}$* mice.

Table S1^{sheet2}. Significantly upregulated genes (P<0.05) in DRG of the *miR^{CKO}* mice.

Table S1^{sheet3}. TargetScan algorithm predicted genes targeted by more than one member of miR-183 cluster.

Table S1^{sheet4}. Total 38 genes carrying binding sites of more than one members of miR-183 cluster and upregulated ⩾1.3 fold. Among these, two were transcription factors which are marked in red (Shox2 and Zbtb41).

Table S1^{sheet5}. The sequences synthesized and cloned in vectors for overexpression of miR-183-96 and miR-182. Underlined are the precursor sequences for each miRNA.

Table S1^{sheet6}. The list of primers used for cloning mouse *Shox2* 3'UTR for luciferase assay and primers for qRT-PCR.

Click here to Download Table S1

Supplementary Reference

Flicek, P., Amode, M. R., Barrell, D., Beal, K., Billis, K., Brent, S., Carvalho-Silva, D., Clapham, P., Coates, G., Fitzgerald, S., et al. (2014). Ensembl 2014. *Nucleic Acids Res* **42**, D749-755.

Larkin, M. A., Blackshields, G., Brown, N. P., Chenna, R., McGettigan, P. A., McWilliam, H., Valentin, F., Wallace, I. M., Wilm, A., Lopez, R., et al. (2007). Clustal W and Clustal X version 2.0. *Bioinformatics* **23**, 2947-2948.

Waterhouse, A. M., Procter, J. B., Martin, D. M., Clamp, M. and Barton, G. J. (2009). Jalview Version 2--a multiple sequence alignment editor and analysis workbench. *Bioinformatics* **25**, 1189-1191.